Unravelling the distribution of decapod crustaceans in the Lower Eocene coral reef mounds of NE Spain (Tremp-Graus Basin, southern Pyrenees)

Fernando A. Ferratges[a]*, Samuel Zamora[b], Marcos Aurell[a]

[a]Departamento de Ciencias de la Tierra-IUCA, Universidad de Zaragoza, E-50009 Zaragoza, Spain ferratges@unizar.es*, maurell@unizar.es

[b]Instituto Geológico y Minero de España, C/Manuel Lasala, 44, 9B, Zaragoza E-50006, Spain s.zamora@igme.es

Abstract

Modern reefs are considered important hot spots of biodiversity, but the analysis of the distribution of the invertebrate fauna across different reefal domains in ancient ecosystems can be challenging because the fossil record is usually affected by strong taphonomic biases. The lower Eocene coral reef in the well-exposed outcrops of Ramals (Tremp-Graus Basin, southern Pyrenees, northeast Spain), preserve a high diversity of invertebrate groups, including decapod crustaceans. In Ramals the reefal facies belt is formed by a 100-200 m width E–W trending facies belt, including a set of closely spaced reef mounds up to five meters high, surrounded by the skeletal-rich (packstones, rudstones) inter-reef facies. These outcrops also allow the analysis of the fossil-association present in the inner and outer fore-reef facies, which are dominated by skeletal packstones with molluscs, foraminifera, corals, bryozoans, decapod

crustaceans, echinoderms and vertebrate fragments (fishes and crocodiles). The reef framework consists of framestones with bioclastic wackestone to packstone matrix, including abundant colonial corals, as well as crustose red algae, encrusting foraminifera (*Solenomeris*), solitary corals and bryozoans. These reef mounds developed within the mesophotic zone, disturbed by the episodic activity of storm-induced waves.

The distribution of decapod crustaceans across the different reefal domains was subjected to extensive paleontological and statistical analyses. The 911 specimens of decapod crustaceans include 41 species belonging to 21 families. Most crustaceans were concentrated in the periphery of the mound reefs and suggest that the core of the reef hosted the highest diversity and abundance of decapod crustaceans. Carpilioids were the most abundant group within the reefal facies belt, *Ctenocheles* sp. dominated the inner fore-reef areas, and *Litoricola macrodactylus pyrenaicus* showed preferences for outer fore-reef environments. Decapod crustaceans and associated faunas lived in close association with coral reefs but disappeared from the area after the demise of the reefs due to the increase of the depositional depth and fine terrigenous sedimentary input, illustrating how diversity changes at local scale due to extrinsic factors.

Key words: Decapoda, coral buildups, paleoecology, taphonomy, Iberian Peninsula.

1. Introduction

The fluctuations in the diversity and abundance of the fossil record of decapod crustaceans and other marine invertebrates which are eventually preserved in shallow

marine facies is dependent on multiple factors, such as sea level changes, ecological factors and preservation processes (e.g. Peters, 2005; Hannisdal and Peters, 2011; Smith et al., 2012; Peters and Heim, 2011; Klompmaker et al., 2013a, b; Dunhill et al., 2014 and references therein; Luque et al., 2019). One example ecological factor is the increase of reef development in certain geological periods, which correlates with the diversity of decapod crustaceans, while drops in decapod diversity coincided with the collapse of reefs several times in Earth history (e.g., Klompmaker et al., 2013b, 2016). Indeed, reefs represent ideal habitats for decapods, providing prevalent shelter and feeding opportunities. In a well-documented case study, the peak of decapod diversity in Albian reefs of the southwestern Pyrenean domain correlated with ecological factors, and was not a preservational artefact (Klompmaker et al., 2013a).

The coralgal reef record around the Paleocene-Eocene transition is scarce, and is dominated by isolated reefs, subordinate to other buildups dominated by calcareous algae and large benthic foraminifera (Rasser et al., 2005; Zamagni et al., 2012; Scheibner and Speijer, 2008; Vescogni et al., 2016). Following the Paleocene-Eocene Thermal Maximum (PETM), the Eocene was a critical epoch in the development of many modern-day features of the Earth, for example palaeogeographical configurations, ocean circulation patterns and several climatic conditions (e.g., Hallock et al., 1991; Hallock and Pomar, 2008; Stickley et al., 2009). Cenozoic Earth surface temperatures attained their warmest state during the early Eocene (Zachos et al., 2001; Payros et al., 2015). In addition, modern-style coral reefs were fully established by the Eocene (see Pomar et al., 2017). These external and ecological factors probably affected the diversification of brachyurans, and consequently many families of modern

species originated in the Eocene (e.g., Brösing, 2008; Tsang et al., 2014; Schweitzer and Feldmann, 2015).

The foreland basins that developed during the Eocene in the southern Pyrenean domain preserve an extraordinary record of shallow marine carbonate successions, including reefs and associated facies (e.g. Pomar et al., 2017; Garcés et al., 2020). In particular, previous studies have addressed the general stratigraphic framework and sedimentary features of the lower Eocene reef mounds exposed in the marginal areas of Tremp-Graus Basin of the southern Pyrenees (i.e. Eichenseer, 1988; Pomar et al., 2017). These previous studies provide the framework forthe characterization of the lower Eocene reef mounds and associated facies in the Ramals outcrop (Tremp-Graus Basin, southern Pyrenees, northeast Spain) performed here.

These Eocene rocks have provided a rich decapod assemblage including anomurans and brachyurans, but few papers have dealt with the relationships between the development of coral reefs and decapod distribution (but see Ferratges et al., 2020 and references therein). Previous studies in Ramals have reported several species of decapod crustaceans (Vía-Boada, 1973; Artal and Vía, 1988; Artal and Castillo, 2005; Fraaije and Pennings, 2006; Artal and Van Bakel, 2018a, 2018b; Ferratges et al., 2019), but none of them focus on the analysis of the distribution of decapods related to the different environments and successive evolutionary stages of the coevally developed reef mounds. The present work provides a well-documented case study demonstrating the relationship between early Eocene reef mound development and coeval setting of an abundant and diverse shallow marine benthic fauna, including a rich association of decapod crustaceans.

The main aims of this work are: (1) to characterize the overall framework and architecture of the coral reef mounds of Ramals, showing the main sedimentological and paleontological features of the associated inter- and fore-reef facies, (2) to describe the relative abundance and diversity of the different groups of marine invertebrates and vertebrates, with particular attention to the characterization of the decapod crustacean assemblages associated to the different reefal environments, and (3) to understand the interaction of the different factors controlling the fluctuations on the diversity of the invertebrate fauna, including decapod crustaceans.

2. Geological setting

The southern Pyrenean Paleogene foreland basins (i.e. Tremp-Graus, Ainsa and Jaca basins) developed in tropical latitudes (e.g. Hay et al., 1999; Silva-Casal et al., 2019). During the Eocene these basins formed part of an elongated gulf connected to the west to the Bay of Biscay and were bounded to the north by the axial zone of the Pyrenees (Plaziat, 1981; Garcés et al., 2020). Sedimentation in these basins has resulted in a well-exposed and complete Eocene succession, showing a great diversity of sedimentary environments, which range from proximal alluvial to shallow marine in the eastern Tremp-Graus basin, to slope and deep marine in most of the Ainsa and Jaca basins, to the abyssal plains of the oceanic basin of the Bay of Biscay (e.g. Garcés et al., 2020).

The lower Eocene reefal unit studied herein is in the middle part of the Serraduy Formation, exposed in the north-western margin of the Tremp-Graus basin. Around the study area of Ramals, the Serraduy Formation forms an almost continuous ESE-WNW trending outcrop (Fig. 1.A). This formation consists of three

lithostratigraphic intervals (Serra-Kiel et al., 1994). The lower member is early Ypresian in age and is traditionally known as *Alveolina limestones.* This unit was deposited after the widespread transgression that occurred at the onset of the Eocene. The topography, together with the warm temperatures, favoured the setting of a low-relief carbonate ramp across the marginal areas of the Tremp-Graus basin at the earliest Eocene, in which the *Alveolina Limestones* was deposited (Ferrer, 1971; Robador et al., 1991; Luterbacher et al., 1991, Eichenseer and Luterbacher, 1992; Payros et al., 2000; Miller et al., 2005; Zachos et al., 2008; Martinius, 2011; Garcés et al., 2020).

The *Alveolina limestones* are overlain by a submarine hard-ground surface, formed after a widespread flooding event. This flooding event reached the marginal areas of the Tremp-Graus basin and was related to the southward migration of the plate flexure (Fonnesu, 1984; Garcés et al., 2020). Low sedimentary rates during this period of sea level rise favoured the development of a hardened surface that allowed the growth of reef mounds variable in size and morphology (Eichenseer and Luterbacher, 1992). These reefs and the associated facies characterize the middle member of the Serraduy Formation studied here (i.e. the *Reef limestones* member; Serra-Kiel et al., 1994). Analysis of the reef framework and the associated facies, combined with the characterization of the associated invertebrate assemblage, indicates that these reefs were developed at deep euphotic to mesophotic depths, around or below storm wave base (Gaemers, 1978; Eichenseer, 1988; Pomar et al., 2017).

The mid-Ypresian deepening event resulted in the eventual flooding of the platform and the sedimentation of *Riguala marls* of the upper part of the Serraduy Formation (Fig. 1). These marls were deposited in a relatively deep, open marine

platform, transitioning to a slope-basin environment, and supported a lower concentration of benthic communities (Serra-Kiel et al., 1994). The *Riguala marls* were dated as lower to middle Ilerdian, which corresponds to the global Ypresian Stage (Pujalte et al., 2009). At a regional scale, most of the studied reef mounds grew over the hardened discontinuity surface found on top of the *Alveolina limestone* (Fig. 1). However, coral-reefs isolated within the *Riguala marls* have been also found near Suerri. There is also the local record of younger coral-reefs in the prodelta marls of the Roda Formation in Bacamorta (Fig. 1).

[Figure 1]

3. Material and methods

Most of the data presented here is based on analysis of fossil specimens collected from the outcrops exposing the *reef limestones* member and the lower part of the *Riguala marls* in the Ramals outcrop (42°18'57"N, 0°32'34"E). The collected specimens are generally recorded in a series of skeletal-rich levels including remains of different invertebrate and vertebrate groups. Further skeletal levels have been sampled westwards and eastwards to Ramals, from the municipalities of Merli to Suerri (see Fig. 1.A). This allowed a broader picture of the overall facies distribution and the recognition of lateral variations related to different reefal environments. Detailed sampling information from these areas is not included in the present study.

Detailed sampling and mapping of the reefs and inter-reef areas around Ramals was performed. This provided information on the geometry and the distribution of the different types of reef facies. Sampling was carried out by surface collecting both in the studied sections and their lateral equivalents. This was accomplished during

approximately thirty field sessions during the years 2018 and 2019, with two researchers expending eight hours per day (average), and the same amount of time in each sampled area. Active extraction and splitting of rocks has been an adequate technique elsewhere for controlled sampling in some reef facies with decapod crustaceans (e.g. Klompmaker et al., 2013a) but was not the case at our fieldwork sites because of the characteristics of the fossil material (the cuticle of crustaceans is not easily visible in fresh fracture), and the siliciclastic nature of the facies. Mapping in Ramals was facilitated by the excellent outcrop condition and supported by aerial photos. The program QGIS 2.18 was used to construct maps. In addition, three stratigraphic successions representative of the different sedimentary domains in the Ramals outcrop were logged and sampled (see Fig. 2 for locations). The characterizations of the reef mound facies are based on field observation combined with core rock sampling around section A, and in a reef mound located in the western part of the outcrop (see P1 in Fig. 2). From these samples, 36 representative thin sections were studied to characterize the microfacies and microfossil association.

The identification of the different sedimentary domains represented in the Ramals outcrop is based in the lateral variation of facies and the recorded fossil assemblages. A thorough sampling of fossil specimens was carried out in the areas of the outcrop representing the reefal facies belt (including the reef mounds and inter-reef facies) and the fore-reef areas. The area located in the transition between the reefal facies belt and the inner fore-reef environment includes the largest abundance of decapods (Fig. 2. A). The invertebrate assemblage and the taxa identified in each domain also helped to support the palaeoenvironmental interpretation.

Remains of a total of 911 decapod crustaceans were collected. Decapods were most commonly recovered as disarticulated carapaces and claws. In general specimens show little abrasion or breakage. Claw remains are usually incomplete, most lack important diagnostic characteristics, and only a few are articulated to a carapace (see exceptions in Artal and Vía, 1988; Artal and Van Bakel, 2018a, 2018b; Ferratges et al., 2019). Although most remains are disarticulated, the cuticle is well preserved, which is uncommon in reef environments (e.g., Klompmaker et al., 2013b, 2016) and allows better identification (Klompmaker et al., 2015). Specimens were counted using the following criteria: (1) carapaces assignable to a specific taxon (from approx.> 30% preserved) were counted as specimens, either at the species level or in open nomenclature; (2) chelae were taken into account only for taxa that preserve this part of the anatomy (i.e., Axiidea and Paguridea). In the case of Axiidea, only the left chelae were counted to avoid overcounting (they correspond to approximately 70% of the total sample for this taxon). In the case of Paguroidea, we only have either left or right chelae for each morphotype so all specimens were counted; (4) the isolated chelae of brachyura (true crabs) were not included because they cannot be assigned with certainty to specific taxa, (5) remaining fragments or appendages were not counted.

The decapod crustacean specimens were prepared using a Micro Jack 2 air scribe (Paleotools) in combination with a microscope. In some cases potassium hydroxide (KOH) was used to remove the matrix. The specimens were then photographed dry and coated with an ammonium chloride sublimate. Detailed photography of the specimens was made using a Nikon D7100 camera (Nikon, Tokyo, Japan) with a macro 60-mm-lens. Specimens were legally sampled under permit EXP: 032/2018 from the *Servicio de Prevención, Protección e Investigación del Patrimonio*

Cultural (Gobierno de Aragón) and deposited in the palaeontological collection of the *Museo de Ciencias Naturales de la Universidad de Zaragoza* under the acronym MPZ (see Canudo, 2018). The exact locations of the different outcrops are marked in Figure 1.

To explore the diversity of the decapod crustacean species distribution in each sedimentary domain chi-squared tests and Principal Component Analyses (PCA) were performed using statistical program Past 4.03 (Hammer et al. 2001). Decapod groups were used as variables of each environment. By performing PCA, the dimensionality of these variables was reduced to determine which were the most characteristic of each environment. To perform these calculations, fossils not assignable to any group (129 specimens corresponding to indeterminate chelae and isolated fragments) were not taken into account. The remaining data were standardized and graphically represented in plots of PC1 vs PC2 and PC1 vs PC3. The information obtained with this method was contrasted with the habits of known taxa to deduce their most probable origin and thus determine whether they correspond to remains transported from adjacent facies (parautochthonous) or if they are characteristic of each facies (autochthonous). The density of each group of decapod crustaceans was calculated by dividing the number of collected specimens by the surface area of the respective zone. The surface areas were calculated using *Iberpix*.

To investigate differences in diversity among zones within the outcrop, multiple measures of diversity were calculated and all samples per site were combined to create an adequate sample size for comparisons among sites. All specimens identified to the species-level were included in the analyses. In addition all taxa that have been identified as different species but left in open nomenclature were included in the

analysis (indeterminate fragments were not used for the analysis). Diversity per site was calculated using the methodology described in Klompmaker et al. (2013a):

"1. Taxa richness: the number of taxa found at each zone.

2. Individual rarefaction curves with 95% confidence intervals were computed for each of the samples using PAST 4.03.

3. Shannon–Wiener Index or Shannon Index or Shannon–Weaver Index $H=-\Sigma pi(\ln(pi))$, where pi is the proportion of the ith species, thus additionally taking into account the number of specimens per species.

4. Margalev's $d=(S-1)/\ln(N)$, where S is the number of species and N is the number of specimens found at the site to account for the fact that more specimens yield more species in general.

5. Simpson's Index of Diversity $=1-(\Sigma n(n-1))/(N(N-1))$, where n is the number of specimens of a species and N again is the total number of specimens found at the site. This measure accounts not only for the number of specimens involved, but also for the number of specimens per species.

6. The Sorensen Index=Si-2c/a+b, where a is the number of species from the zone 1, b is the number of species from the zone 2, and c is the number of species that share two zones. This measure has been used to determine the degree of similarity between zones.

7. The Chao1 Index (Chao, 1984) estimator of the absolute number of species in an assemblage: SChao1=Sobs+(F12/2F2), where Sobs is the number of species in the sample, F1 is the observed number of species represented by one specimen, and F2 is the observed number of species represented by two specimens. This measure

calculates the theoretical number of species if an infinite number of specimens had been collected.

8. Pielou's evenness index was also calculated: E=H/ln(S), where E is the evenness index and H is the Shannon Index (see above)."

[Figure 2]

4. The reef mounds and associated facies

The reconstruction of the lateral relationship of the reef, inter- and fore-reef facies characterized in the outcrop exposed around Ramals provided the overall sedimentological and stratigraphic framework, in which the different collected decapod crustacean assemblages are located. The three logged and sampled stratigraphic sections (Fig. 3) cover the reef facies (section A), the inner fore-reef facies (section B) and the outer fore-reef facies (section C), as well as the basal levels of the post-reefs facies (*Riguala marls*, sections B and C).

In the northern part of the Ramals outcrop, a set of closely spaced reef mounds form a 100-200 m wide E–W trending belt (Fig. 2.A). The reefs consist of isolated or agglutinated mounds up to five meters high. They sit directly on over the hardground surface that developed on top of the *Alveolina limestones*. In addition, the initial growth of some of these reefs can be related to local step faults (Fig. 2-P1).

The reef framework consists of coral framestones with bioclastic wackestone to packstone matrix (Fig. 4). Coral colonies are rarely preserved in growth position within the reef framework, indicating the episodic activity of currents, probably related to storm-induced waves. The reef is dominated by massive and tabular colonies, represented by the genera *Actinacis*, *Astreopora*, *Colpophyllia* and *Cyathoseris*.

Branching colonies (such as the genus *Actinacis*) are also abundant. Other identified colonial corals include *Stylocoenia*, *Astrocoenia, Agaricia* and *Caulastraea*. Solitary corals (*Placosmilopsis, Leptophyllia*) are also found. Other relevant organisms that helped to build the reef framework are crustose coralline red algae, encrusting foraminifera (*Solenomeris*) and bryozoans (Figs. 4-B, C and 5-B, E).

At some points the reef mounds overlapped and growing over each other. This allowed the accumulation of sediments underneath them (Fig. 2-P2). At other points sediment accumulated in inter-reef spaces (Fig. 2-P3). These inter-reef areas include a large number of redeposited bioclastic levels with poorly sorted rudstone to packstone textures (Fig. 5.B, C, D), with a relative abundance of glauconite. The areas attached to the pinnacles include large blocks of coral reef framework rubble. The branching colonies (such as the genus *Actinacis*) are particularly abundant in the rubble redeposited in the skeletal-rich levels found a few tens of meters away in the main reefal facies belt.

The central and southern part of the Ramals outcrop corresponds to deeper fore-reef areas, in which reef mounds are absent and the proportion of skeletal grains is lower, resulting in wackestone to packstone textures (Fig. 2). The inner fore-reef facies attached to the northern reefal facies belt, consists of decimetre-thick rudstone to packstone levels interbedded with bioclastic marls, and contains a great abundance and diversity of fossils (Fig. 5.D, E, F). These coarse-grained and poorly sorted skeletal levels gradually pass to finer-grain skeletal packstone beds that eventually pinch out offshore (southwards), further away from the reef. This lateral gradation indicates that most of the skeletal components found in these levels were sourced from the reef mounds, and were transported downslope, most probably by storm-induced currents.

The inner fore-reef facies grade upwards to finer-grain bioclastic beds (decimetre-thick wackestone and packstone), with intercalated marls. These levels contain a low diversity, composed mostly of bivalves (ostreids), gastropods and occasionally echinoderms and decapods. The decrease in grain size and increase of muddy matrix up section indicates a decrease in hydrodynamic energy, probably related to the coeval increase in the depth of deposition.

Southwards, the outer fore-reef deposits are reduced to less than one meter (Fig. 3, section C). These deposits are mostly formed by skeletal packstones dominated by benthic foraminifera (Fig. 5F, G). There is some significant lateral variation in the dominant skeletal grains compared to the inner fore-reef facies. As a general rule, the diversity and concentration of skeletal debris is lower in the outer fore-reef areas, and there is a rapid decrease in the abundance and diversity of invertebrate fossils. The lateral variation on the recorded invertebrate fossil association across the fore-reef domains indicates that these skeletal levels are in fact a mixture of redeposited (parautochthonous) and autochthonous material.

The sedimentation of the *Riguala marls* occurred after the demise of reef mounds. These post-reef facies onlap and cover the reefs and associated bioclastic facies, and show an important decrease in the number of benthic fossils. The marls include interbedded decimetre-thick fine-grained detrital levels with scarce skeletal grains, which pinch out laterally towards the South.

[Figure 3]

[Figure 4]

[Figure 5]

5. The fossil association of the reefal facies belt

The analysis of the skeletal grains recorded in the inter- and fore-reef facies provided precise information about the fossil groups that developed coeval to the coral reef mound development. Among these groups are molluscs, foraminifera, corals, bryozoans, decapod crustaceans, echinoderms and vertebrates (see Figs. 6 and 7). The diversity and abundance of the recorded fossil assemblage indicates a favourable environment for the development of the benthic fauna while the reef was actively growing. The remains of decapods and other marine invertebrate groups are frequently disarticulated and fragmented, with local colonization by epibenthic fauna. In the case of decapods we cannot discard the possibility that some epibionts (mostly serpulids) attached during life, but in the case of echinoids most epibionts attached post-mortem because they affected parts originally covered with spines (Fig. 6). About 40 percent of echinoids were colonized by epibionts.

5.1. Decapod crustaceans

Decapod crustaceans were abundant both in the inter-reef and fore-reef environment (table 1). A total of 41 different decapod species were recognized that are included in 21 families: Callianassidae, Ctenochelidae (Axiidae); Diogenidae, Paguridae (Anomura); Basinotopidae, Dynomenidae, Sphaerodromiidae, Homolidae, Raninidae, (podotreme brachyurans); Aethridae, Calappidae, Goneplacidae, Matutidae, Carpiliidae, Hexapodidae, Pilumnidae, Panopeidae, Parthenopidae, Portunidae, Tumidocarcinidae, Xanthidae (heterotreme brachyurans). This decapod assemblage has similarities with material collected from other European localities

associated with Eocene reef facies (see, e.g., Beschin et al., 2007, 2015; Tessier et al., 2011).

5.2. Echinoderms

Among the echinoderms, marginal plates of goniasterid asteroideans (?*Calliderma* sp.; Fig. 6 V) and abundant crinoids were found (*Bourgueticrinus* sp.; Fig. 6 W-X) (see Zamora et al., 2018). In the studied area, these levels provided a great diversity of regular and irregular echinoids (Bataller, 1937; Gurrea, 1999; Carrasco, 2003, 2006, 2015, 2017). Among them (Fig. 6), the following taxa of regular echinoids were identified: *Ambipleurus* sp., *Baueria angelae* Carrasco, 2006; *Arachniopleurus reticulatus* Duncan & Sladen, 1882; *Fellius pouechi* (Cotteau, 1863); *Cidaris gourdoni* Cotteau, 1889; ?*Thylechinus frossardi* (Cotteau, 1889); *Salenia* sp.; Irregular echinoid fauna includes: *Ditremaster nux* (Desor, 1853); *Eurhodia* sp.; *Maretia arogonensis* (Cotteau, 1887); *Trachyaster* sp.; *Cyclaster gourdoni* (Cotteau, 1887); *Linthia aragonensis* (Cotteau, 1887); *Linthia hovelacquei* Cotteau, 1889; *Amblypygus dilatatus* Agassiz, 1840; *Echinocyamus* sp.; *Echinolampas leymeriei* Cotteau, 1863; *Echinolampas* sp.; *Gitolampas cotteaui* (Hébert, 1882); *Holcopneustes* sp.; *Prenaster* sp.; *Pygorhynchus aragonensis* Cotteau, 1889; *Schizaster rousseli* Cotteau, 1887; *S. vicinalis* (Agassiz and Desor, 1847).

5.3. Foraminifera, other invertebrates and vertebrate remains

The foraminifera include both benthic (free-living and encrusting) and planktonic forms. The species of benthic foraminifera were identified as discocyclinids (Figs 4.C and 5), assilinids (?*Heterostegina*), *Alveolina*, orthophragminids, textularids

(biseriate?), fiserinids, *Operculina*, *Nummulites*, possibly Discorbidae, ?*Amphistegina*, *Gibsina* (?*Esferogibsina*), and abundant rotalids (of different species), *Solenomeris* (Fig. 4.B), *Acervulina* sp. (Figs. 4.C) and miliolids (Fig. 5).

Gastropods were found in great abundance (Cypraeidae, Xenophoridae, Fasciolariidae, Rostellariidae, Naticidae and Neritidae), most preserved as internal moulds. Epifaunal and infaunal bivalves were also identified. Epifaunal bivalves include groups with a free mode of life (Spondylidae, Chamidae, Pectinidae) and some that cemented to hard substrates (Ostreidae). Among the infaunal bivalves, taxa adapted to different substrates were found, like Mytilidae (*Lithophaga*) for hard substrates; Cardiidae, Carditidae, Lucinidae, Crassatellidae and Pinnidae for soft substrates; and *Teredolites* for wood substrates (Carrasco, 2004).

In addition, several species of terebratulid, ostracods (Fig. 5 D-H), bryozoans (Fig. 5 B-F) and serpulids were found. Some internal moulds of large nautiloids (larger than 30 cm), probably of the genus *Eutrephoceras*, and parts of their mouth apparatus (*Rhyncholites* sp.; Fig. 6 D) were also retrieved. In some cases, the shell of these nautiloids were associated with other organisms, which used these shells for shelter (Fraaije and Penning, 2006).

Fish remains, mainly teeth of sharks and rays, indeterminate bones, otoliths and teeth of teleost fishes, rostral fragments of *Cylindracanthus* sp. and isolated bones of Crocodylia indet. (Eusuchia indet.) were less abundant (Fig. 6). The single specimen of Crocodylia indet. was encrusted by oysters and bryozoans.

[Figure 6]

[Figure 7]

6. Palaeoenvironmental interpretations

A palaeoenvironmental reconstruction is provided for the shallow marine carbonate platform that developed during the early Eocene (middle Ypresian) around the Ramals area, in the northern margin of the Tremp-Graus basin (Fig. 8). Two stages of platform evolution were differentiated. A first stage with coral reef mound development involved a great abundance and diversity of the invertebrate marine fauna (Fig. 8 A). The paleoenvironment in which the reef mounds and inter-reef facies developed (reefal facies belt, see 1 in Fig. 8 A) grades offshore to the fore-reef setting (i.e., the inner- and outer fore-reef facies; see 2 and 3 respectively, Fig. 8 A). Abundance gradually decreases from the reefal facies belt to the outer fore-reef setting.

The first stage favourable for reef development coincides with a period of relative tectonic stability in which there was a low, fine-grained, terrigenous clastic input. These conditions had to be maintained long enough to allow the growth of reef mounds several meters in diameter. At the onset of the second stage, sedimentation rate and depositional depth increased suddenly (Fig. 8.B), probably due to an increase in tectonic activity. A deepening platform combined with an increase of terrigenous input due to the progradation of a deltaic system that moved westward in the Tremp-Graus basin (Serra-Kiel et al., 1994), to trigger the rapid disappearance of the reef and the collapse of the reef-induced ecosystem.

During the reef stage, the presence of assilinids, *Discocyclina* and planktonic foraminifera, combined with the absence of the typical inner platform organisms (such as green algae), suggest that the reefal facies belt developed in the euphotic to mesophotic zone, below the normal-wave base zone but above storm-wave base level

(Scheibner et al., 2007; Morsilli et al., 2012; Pomar et al., 2017). This is further supported by the presence of *Solenomeris* in the reef framework, which is a relatively deep-water foraminifer (Plaziat and Perin, 1992). In addition, the abundance of encrusting red algae within the reef framework is an indicator of deeper waters than reefs predominantly composed by corals (e.g., Baceta et al., 2005).

The diversity and abundance of benthic groups coeval to the reef development indicates that the seabed was rich in nutrients, thus allowing the presence of organisms feeding at different levels of the trophic scale: primary producers (such as red algae), suspension feeders (brachiopods, corals, crinoids, etc.), detritivores (some irregular echinoids), primary consumers (regular echinoids), scavengers and active predators (mainly fish, crocodiles and decapods).

Coral colonies are rarely preserved in growth position within the reef framework. Waves and storm-induced currents broke the coral colonies, which accumulated as rubble in the inter reefs areas, but also over the reef substrate (Massel and Done, 1993; Madin and Connolly, 2006). These high-energy events limited the presence of mechanically unstable corals, and allowed a great diversity of other corals to continue to grow (Connell, 1978). These mechanically unstable coral species, susceptible to waves, offered more shelter and food for other organisms (Madin et al., 2012).

The relative abundance of glauconite in the inter-reef facies, along with the mode of preservation of the skeletal grains suggests that sedimentation rates were low. Further support for reduced sedimentation rates is provided by the presence of encrusting foraminifera such as *Acervulina* (see Scheibner et al., 2007) and epibionts on post-mortem echinoid skeletons (Fig. 6G). The bioclastic material produced in the

reef was transported by storms to the fore-reef area where most of the studied fossils were found, commonly disarticulated and often fragmented. The low abundance of articulated material is explained by long periods of exposure on the seafloor to storm-induced waves and currents, which resulted in the fragmentation and disarticulation of decapods and other marine invertebrate groups (i.e., Mutel et al., 2008; Krause et al., 2011; Klompmaker et al., 2015, 2017). Low sedimentation rates also explain the colonization by epibenthic fauna of echinoid skeletons following the disarticulation of their spines.

The degree of degradation that a specimen presents can provide clues to the mechanism of transport, scavenging and other factors (Mutel et al., 2008). The state of preservation of the crustacean remains found in the studied area can be explained, at least partially, from the taphonomic studies carried out by some authors (Jakobsen and Feldmann, 2004; Mutel et al., 2008; Krause et al., 2011; Klompmaker et al., 2017). Most decapod crustacean remains are limited to the cephalothorax or isolated chelae, with only few examples preserving partial articulated specimens (Artal and Vía, 1988; Artal and Van Bakel, 2018a, 2018b; Ferratges et al., 2019). The collected remains, both of decapod crustaceans and echinoderms, suggest a relatively complex taphonomic history, with re-sedimentation events and long periods of exposure in the water-sediment interface that lengthened the biostratinomic phase (e.g., Nebelsick, 2004; Smith and Rader, 2009; for echinoderms; Allison, 1986; Mutel et al., 2008; Parsons-Hubbard et al., 2008; Krause et al., 2011; for decapods). Occasional high-energy events, which were not enough to completely destroy relatively delicate specimens, transported material to the inter- and fore-reef areas where it was finally buried.

[Figure 8]

7. Abundance and distribution of decapod crustaceans

The decapod assemblage collected in Ramals corresponds largely to taxa associated with reef environments. The most abundant genus in the reefal complex is *Ctenocheles* (55.10 per cent), followed by representatives of the superfamily Xanthoidea (5.27 per cent), paguroids (5.49 per cent), *Ilerdapatiscus* (5.05 per cent) and carpilioids (3.74 per cent). Minor components include some species of dromioids (1.98 per cent), portunoids (1.43 per cent), parthenopoids (genus *Aragolambrus*) (0.66 per cent), calappoids (0.55 per cent), raninoids (0.55 per cent), pilumnoids (0.44 per cent), and remains of homoloids (0.22 per cent).Two independent taxa were represented by a single specimen each (0.22 per cent) and 129 isolated remains could not be assigned with confidence to any group (14.16 per cent of the total sample) (see Table 1).

Other localities in the Eocene of Europe have broadly similar carcinologic associations in terms of diversity and abundance (see e.g., Beschin et al., 2007, 2015, 2018; Tessier et al., 2011). However, the exceptional state of preservation of the Ramals outcrop and its optimal exposure in three dimensions, allowed a detailed sampling of different lithofacies and different sectors of the reefal environment. This allowed the quantification of the appearance of each taxon and study of its lateral and vertical variation. The number and diversity of decapod crustaceans in the studied area is not random. Faunal changes were observed from the three sampled intervals (reefal facies belt, inner- and outer fore-reef facies; Fig. 9).

[Table 1]

[Figure 9]

The reefal facies belt, including the reef mounds and adjacent inter-reef areas (Fig. 8 A-1) has an intermediate diversity and the lowest abundance of decapod crustaceans (Table 2 and Fig 9). In this lithofacies, the dominant group is the carpilioids (37.9 per cent) followed by paguroids (17.24 per cent), *Ctenocheles* (13.79 per cent), aethroids (10.34 per cent), pilumnoids (10.34 per cent), xanthoids (6.9 per cent) and dromioids are very rare (3.45 per cent) (Fig. 9). Several unidentified chelae have also been found, representing 58.32 per cent of the total assemblage. These are difficult to identify at the species level because they correspond mainly to disarticulated and broken fragments.

The inner fore-reef facies (Fig. 8 A-2) hosts the greatest diversity and abundance of decapod crustaceans (Fig. 9) and is mainly composed of small crabs. The most abundant taxon is *Ctenocheles*, only represented by fragments of chelipeds, representing 65.51 per cent of the sample, followed by paguroids (8.37 per cent), aethrioids (*Ilerdapatiscus*) (7.55 per cent), some species of xanthoids (6.94 per cent), carpilioids (3.88 per cent), dromioids (3.27 per cent), parthenopoids (*Aragolambrus*) (1.02 per cent), raninoids (1.02 per cent), calappoids (0.82 per cent), portunoids (0.61 per cent), homoloids (0.41 per cent), pilumnoids (0.2 per cent), hexapoids (0.2 per cent) and goneplacoids (0.2 per cent). There are also abundant remains of several indeterminate taxa, which represent 15.09 per cent of the total assemblage (Table 1).

The outer-fore reef facies (Fig. 8.A-3) shows the lowest diversity and intermediate abundance (Table 1). In this lithofacies, the most abundant taxon is represented by fragmented claws of *Ctenocheles* (47.54 per cent) followed by *Litoricola macrodactylus pyrenaicus* (16.39 per cent). Minor components belonging to

seven different families represent the remaining 36.07 per cent (Table 2). Indeterminate taxa represent 21.11 per cent of the total assemblage.

[Table 2]

The faunal distribution of decapods in Ramals shows important differences in terms of both relative abundance and diversity in each of the differentiated facies belts. In order to explore if there was a relationship among the distribution of the species in each facies, a Principal Component Analysis (PCA) was performed. To simplify the calculations, the different recognized taxa were grouped into superfamilies (Table 2). Taking these groups as variables, we were able to infer which groups had preferences for a specific environment. The three main principal components (PC1, PC2 and PC3) are visualised in Figure 10.

By reducing the dimensionality of variables using PCA, it is shown that certain taxa have strong affinity for particular environments. For example carpilioids occupy a position in the top left of the plot of PC1 against PC2, indicating a much more positive PC2 value compared to other groups. This is mainly explained by the diversity of this group in the reefal facies belt environment (Fig. 10 A). It can also be observed that the portunoids (specifically the species *Litoricola macrodactylus pyrenaicus*) occupy a position in the top left of the plot of PC1 against PC3, indicating a much more positive PC3 compared to the other groups. This is mainly explained by the diversity of this group in outer-fore reef facies (Fig. 10 B). Also notable is the distribution of Axiidea which is markedly much more positive on the PC1 axis than any other group. This is mainly explained by the diversity of this group in inner fore-reef facies (Fig. 10 A and B). The distribution (and high concentration) of Axiidea is not surprising, because members of this infraorder are mostly represented by *Ctenocheles*, considered a

bioturbator taxon typical of soft or sandy bottoms of shallow waters (i.e. Hyžný and Klompmaker, 2015 and references therein).

On the other hand, the remaining groups are more or less clustered in PCA space (Fig. 10). Thus, groups such as Pilumnoidea, Xanthoidea, Paguroidea, and Aethroidea show a trend resulting from their reef facies belt facies (positive in PC 2) (Fig. 10 A). Similarly, Dromioidea, Parthenopoidea (*Aragolambrus*), Calappoidea and Raninoidea are more representative of the inner fore-reef facies (positive in PC1) (Fig. 10 A and B). Some groups may show a greater dispersion to the outer fore-reef facies (for example Aethroidea, Xanthoidea and Axiidea). This may be because they are the more abundant taxa and therefore easier to collect during the sampling, but we cannot discount that these groups were more widespread in different facies. In contrast, the only taxon showing complete and articulated specimens in the outer fore-reef facies is *L. macrodactylus* suggesting rapid burial by episodically high sedimentary events. This taxon probably lived in this area.

To demonstrate that some areas contained more specimens of certain groups than others, the number of specimens in each group was normalized, and their densities calculated. The number of specimens was divided by the total area of the different sampling zones. Following this normalization, areas of higher abundance of some groups than others can be determined. The values obtained for the density of decapod crustaceans in each sector of the outcrop vary by one or two orders of magnitude (Table 3), which supports the idea that some groups showed preferences for facies type. For example the density of Axiidea and Dromioidea varies by two orders of magnitude, suggesting that these groups are strongly linked to inner fore-reef facies.

[Fig. 10]

[Table 3]

Several analyses (see below) were performed in order to investigate links between diversity with type of facies. Our null hypothesis (H_0) was that species composition does not differ between facies (Table 4). The alternative hypothesis (H_1) was that species composition does differ between facies. The p-values of chi-squared tests were < 0.05 in all cases (reefal facies vs inner fore-reef facies: 4.84E-13; reefal facies vs outer fore-reef facies: 3.05E-4; and inner fore-reef facies vs outer fore-reef facies: 1,37E-06), which suggests that there is a significant link between species and the different facies (acceptance of H_1). Both the PCA and the pie-charts clearly reflect that it is mainly carpilioid taxa that differentiate the reefal facies. The PCA and the pie-charts indicate that the raninoids and a greater relative abundance of Axiidae are characteristic of the inner fore reef. Differences and relative abundances of portunoids characterize the outer fore reef.

[Table 4]

8. Discussion: Taphonomic biases affecting decapod crustacean diversity

The data compiled from the lower Eocene outcrop of Ramals confirms that the coral reef mounds which grew in the relatively shallow warm waters (mesophotic zone), combined with episodic storm-wave reworking, provided a favourable conditions for the development of a diverse and abundant decapod assemblage. This diversity suddenly dropped after the reef mounds were drowned and covered by sediments -the *Riguala marls* (Fig. 8B)- only a single species of decapod (*Litoricola macrodactylus pyrenaicus*) remained. The loss of capacity of the environment to

sustain a rich and complex ecosystem is explained by the disappearance of ecological niches offered by the reef due to sediment clogging.

The Ramals outcrop offers an excellent opportunity to discuss the interplay of factors preserving fossil decapod communities affected by different taphonomic processes in different facies. Depending on the depositional processes and taphonomic bias, decapod remains can be preserved close to their living site (e.g., Allison, 1986; Krause et al., 2011). Disarticulated carcasses or exuviae of crustaceans can be exposed in the sediment-water interface for long periods of time without degrading (Allison, 1986, 1988; Plotnick, 1986; Briggs and Kear, 1994; Martel et al., 2008; Parsons-Hubbard et al., 2008; Krause et al., 2011; Klompmaker et al., 2017). In the case of "burrowing shrimp" (Callianassidae and Ctenochelidae), only the hardened parts are preserved (i.e., the chelae), due to the delicate nature of the rest of the cuticle (Hyžný and Klompmaker, 2015; Klompmaker et al., 2017). In the case of the Ramals reefal facies belt , the state of preservation and the sedimentological data suggest that most specimens were exposed for long periods of time before burial. This is also supported by observations in other invertebrate groups like echinoids, that appear colonized by serpulids and bryozoans, suggesting a prolonged residence time on the sediment-water interface (Nebelsick and Kroh, 2002; Nebelsick, 2004). Furthermore, some vertebrate bones were colonized by oysters and bryozoans.

Preferential preservation occurred mostly in inner fore-reef facies. This environment hosts the greatest abundance and diversity of decapods in Ramals, and this is probably correlated with the most favourable taphonomic conditions. This facies belt accumulated most of the bioclastic sediment transported by episodic storm-induced currents, and hosted autochthonous and parautochthonous taxa that lived

within the reef and in the soft sediment of the attached fore-reef domain. This is the case of some decapods, whose modern relatives are adapted to soft substrates like raninoids (e.g. Goeke, 1985; Kasinathan et al., 2007) and Axiidae (Fig. 7 A-C) (e.g., Dworschak, 2000, 2005; Hyžný and Klompmaker, 2015). Other taxa were adapted to live among coral rubble, like the genus *Aragolambrus* (Ferratges et al., 2019) and calappoids (e.g. Schweitzer and Feldmann, 2000).

The low diversity and abundance of fauna in the reefs and inter-reef areas is probably related to taphonomic factors. This sedimentary domain represents areas of high energy and low preservation potential of crustacean decapods. Mainly carpilioids, some aethrids (*Ilerdapatiscus*), rare dromioids and fragments of chelipeds have been found, whereas most of the autochthonous fauna was probably transported to the inner fore-reef facies belt (Fig. 8-A).

Finally, the outer fore-reef facies recorded the lowest sedimentation rates, although episodically affected by distal storm events, and also hosted the lowest diversity of decapods, including *Litoricola macrodactylus pyrenaicus* (Artal and Vía, 1988); *Ctenocheles* sp.; xanthoids; rare dromioids and fragments of indeterminate chelipeds. All fossil remains from these facies, except those belonging to *Litoricola macrodactylus pyrenaicus*, are disarticulated and often broken, so it can be deduced that most of the fauna from this interval was probably transported from proximal facies. The specimens of *L. macroactylus* are an exception, and they are completely preserved, with carapaces articulated to chelipeds and locomotory legs. In addition, this species was the only one found in the post-reef sediments, suggesting that it did not have a close relationship with coral environments.

Species that are always found in all zones are *Ctenocheles* sp., *Ilerdapaticus guardiae* Artal and Van Bakel 2018a, *Eocarpilius ortegai* Artal and Van Bakel 2018b, *Carpilius* sp., and *Xanthilites* sp. (Fig. 7; Table 1). *Ctenocheles* sp. is the most common species in all zones, except for reefal facies where *Carpilius* sp. is represented by eleven specimens (Table 1).

Although the rarefaction analysis indicates that sampling has not stabilized (Fig. 11), the curves of the three zones have stopped growing exponentially, and indicate a different stabilization point in each zone. Based on our sampling and the Shannon index, the data obtained suggests that the greatest diversity is concentrated on the reefal facies (Fig. 12). On the other hand our sedimentological analysis suggests that most specimens from the core reef were transported to the inner fore-reef facies by storm events. Taken together, these lines of evidence could explain why some taxa are represented by a small number of individuals (see Fig. 9 and Fig. 11).

[Fig. 11]

[Fig. 12]

The Chao1 index (Fig. 13), which estimates abundances, is highest in the inner fore-reef. However, the fact that several taxa are represented by a low number of specimens suggests that these taxa have been transported from the core reef. Tables 1 and 2 shows that inner fore-reef facies contained the highest number of species. Thus, based on a variety of diversity measures our hypothesis is that inner fore-reef facies preserved the most abundant assemblage; although some species preserved in such zone were transported from the core of the reef. However, for the Simpson's Index of

Diversity and Shannon–Wiener Index, the inner fore-reef facies came in third and second position respectively (Table 4). These indices are highest for the reefal facies.

The Shannon index measures specific biodiversity. Our study areas show a Shannon index of 2.225 for the reefal facies, 1.7 for the inner fore-reef, and 1.644 for the outer fore-reef (see Table 4 and Fig. 12), showing that the zone with the greatest diversity of taxa corresponds to the reefal facies. In order to compare whether these differences in the Shannon index are significant between the studied areas we performed a T test. Comparisons of the reefal facies vs the inner fore-reef and the reefal facies vs outer fore-reef facies (see supplementary material), resulted in *P* values of 0.001 and 0.003 respectively. The *P* value in both cases falls below the significance threshold (0.05) and thus indicate significant differences between the facies. On the other hand, a comparison of the inner fore-reef vs outer fore-reef, resulted in a *P* value of 0.735, which indicates that the differences in the Shannon index obtained in the inner- and outer fore-reef are not significant. In terms of evenness, all sites have an evenness ranging from 0.14 to 0.841, which implies that more than one species are important contributors to the decapod diversity at each zone (Table 4).

[Fig. 13]

9. Conclusions

The lower Eocene (Ypresian) outcrop of Ramals (Graus-Tremp basin, southern Pyrenees, Spain) exposes a reefal facies belt including closely spaced mounds up to five meters high, and associated inter- and fore-reef facies. The reef framework consists of coral framestones with bioclastic wackestone to packstone matrix, with colonial corals (*Stylocoenia*, *Astrocoenia, Astreopora, Agaricia, Actinacis, Cyathoseris, Colpophyllia*

and *Caulastraea)*, solitary corals (*Placosmilopsis, Leptophyllia*), crustose red algae, encrusting foraminifers (*Solenomeris*) and bryozoans.

The reef mounds and associated facies developed within the euphotic to mesophotic zone (a few tens of meters deep), with some nutrient content to maintain the diversity of associated benthic organisms. Evidence of episodic activity of storm-induced waves and currents is provided by abundant coral rubble within the reef framework and the skeletal-rich beds accumulated on the inter- and fore-reef domains. These beds are dominated by molluscs, foraminifera, corals, bryozoans, decapod crustaceans, echinoderms and vertebrate fragments. The presence of epibionts in some skeletal remains (such as echinoderms and fragments of vertebrates) indicates long periods of time on the sea floor.

The studied reef mounds and associated facies allowed the establishment of a rich association of decapods consisting of 41 species. These are mostly preserved as claw fragments or isolated carapaces, although little abrasion or breakage has been observed. A Principal Component Analysis (PCA) suggests that superfamilies were distributed across different facies. Thus, in the reef and inter-reef areas, the most representative groups are: Carpilioids, pilumnoids, xanthoids, *Ilerdapatiscus* and paguroids; the inner fore-reef are dominated by Axiidae, dromioids, parthenopoids, calappoids and raninoids; in the outer fore-reef area, the most representative taxon is *Litoricola macrodactila pyrenaicus*. The only decapod that remained in the post-reef marls deposited after the collapse of the reef mounds is *Litoricola macrodactylus pyrenaicus*.

Statistical analyses of diversity indicate that the studied areas are significantly different, corroborating the sedimentological analysis. These analyses also strength the

hypothesis that the greatest diversity was found in the reefal facies belt and that an important part of the generated remains in such area were transported to fore reef facies.

Acknowledgements

This work has been supported by the projects CGL2017-85038-P subsidized by the Spanish Ministry of Science and Innovation, the European Regional Development Fund, and Project E18-20R *Aragosaurus: Recursos Geológicos y Paleoambientes* of the government of Aragón-FEDER. The research of Fernando A. Ferratges is funded by a FPU Grant (Spanish Ministry of Science and Innovation). The authors would like to acknowledge the use of *Servicio General de Apoyo a la Investigación-SAI, Universidad de Zaragoza*. We thank Vanessa Villalba-Mouco for her suggestions and help with statistical analyses, Pedro Artal for his help with the identification of decapods, and Carme Boix, Erzica Crúz and Esmeralda Caus for their help and advice with the interpretation and identification of foraminifera. We thank Eduardo Puértolas for the identification of the crocodile remains. Isabel Pérez provided photography assistance. Finally, we are grateful to the journal reviewers, Adiël Klompmaker (University of Alabama), Javier Luque (Harvard University) and an anonymous reviewer, and the handling editor, for pertinent and exhaustive comments on an earlier version of this manuscript. Adiël Klompmaker also provided important discussions on the statistical treatment of our data. Stephen Pates (University of Cambridge) did a deep grammatical review of the present work.

Declaration of interests

☒ The authors declare that they have no known competing financial interests or personal relationships that could have appeared to influence the work reported in this paper.

References

Agassiz, L., 1840. Catalogus systematicus Ectyporum Echinodermatum fossilium Musei Neocomensis, secundum ordinem zoologicum disposi us; adjectis synonymis recentioribus, nec non stratis et locis in quibus repe iunt ur; sequuntur Characteres diagnostici generum novorum vel minus cognitorum. Apud Oliv. Petitpierre, Neuchâtel, pp. 1–20.

Agassiz, L., Desor, P.E., 1847. Catalogue raisonné des familles, des genres et des espèces de la classe des échinodermes. Ann. Sci. Nat. Zool. Biol. Anim. 8, 355–380.

Allison, P.A., 1986. Soft-bodied animals in the fossil record: the role of decay in fragmentation during transport. Geology 14, 979–981. https://doi.org/10.1130/0091-7613(1986)14<979:SAITFR>2.0.CO;2.

Allison, P.A., 1988. The role of anoxia in the decay and mineralization of proteinaceous macro-fossils. Paleobiology 14, 139–154.

Artal, P., Castillo, J., 2005. *Cyrtorhina ripacurtae* n. sp. (Crustacea, Decapoda, Raninidae), primera cita del género en el Eoceno inferior español. Batallería 12, 33–38.

Artal, P., Van Bakel, B., 2018a. Aethrids and panopeids (Crustacea, Decapoda) from the Ypresian of both slopes of the Pyrenees (France, Spain). Scripta Musei Geologici Seminarii Barcinonensis 22, 3–19.

Artal, P., Van Bakel, B., 2018b. Carpiliids (Crustacea, Decapoda) from the Ypresian (Eocene) of the Northeast of Spain. Scripta Musei Geologici Seminarii Barcinonensis 22, 20–36.

Artal, P., Vía, L., 1988. *Xanthilites macrodactylus pyrenaicus* (Crustacea, Decapoda) nueva subespecie del Ilerdiense medio del Pirineo de Huesca. Batalleria 2, 57–61.

Baceta, J.I., Pujalte, V., Bernaola, G., 2005. Paleocene coralgal reefs of the western Pyrenean basin, northern Spain: newevidence supporting an earliest Paleogene recovery of reefal systems. Palaeogeogr. Palaeoclimatol. Palaeoecol. 224, 117–143. https://doi.org/10.1016/j.palaeo.2005.03.033.

Bataller, J.R., 1937. Catàleg de les espècies fòssils noves del cretàcic de Catalunya i d'altres regions. Arxius de l'Escola Superior d'Agricultura 3, 581–619.

Beschin, C., Busulini, A., De Angeli, A., Tessier, G., 2007. I decapodi dell'Eocene inferior di Contrada Gecchelina (Vicenza – Italia settentrionale) (Anomura e Brachiura). Mus. Archeol. Sci. Nat."G. Zannato" Montecchio Maggiore (Vicenza). 9–76.

Beschin, C., Busulini, A., Fornaciari, E., Papazzoni, C.A., Tessier, G., 2018. La fauna di crostacei associati a coralli dell'Eocene superiore di Campolongo di Val Liona (Monti Berici, Vicenza, Italia nordorientale). Boll. Mus. St. nat. Venezia. 69, 129–215.

Beschin, C., Busulini, A., Tessier, G., 2015. Nuova segnalazione di crostacei associate a coralli nell'Eocene inferiore dei Lessini Orientali (Vestenanova-Verona). Lavori Soc. ven. Sci. nat. 40, 47–109.

Briggs, D.E., Kear, A.J., 1994. Decay and mineralization of shrimps. Palaios 9(5), 431–456.

Brösing, A., 2008. A reconstruction of an evolutionary scenario for the Brachyura (Decapoda) in the context of the Cretaceous-Tertiary boundary. Crustaceana 81(3), 271–287. https://doi.org/10.1163/156854008783564091.

Canudo, J.I., 2018. The collection of type fossils of the Natural Science Museum of the University of Zaragoza (Spain). Geoheritage 10, 385–392.

Carrasco, J.F., 2003. Presencia de la icnoespecie *Gnathichnus pentax* sobre *Dimya richei* (Bivalvia) en el Eoceno inferior de La Puebla de Roda (Huesca). Batalleria 11, 37–40.

Carrasco, J.F., 2004. Aportaciones al conocimiento de la icnoespecie *Teredolites longissimus* (Fm. Serraduy. Eoceno inferior de la zona surpirenaica central). Batalleria 12, 61- 74.

Carrasco, J.F., 2006. Una nueva especie del género Baueria (Echinoidea) del Eoceno inferior de la cuenca de Tremp-Graus (Zona central surpirenaica). Scripta Musei Geologici Seminarii Barcinonensis 1, 19–34.

Carrasco, J.F., 2015. Primera cita de Gitolampas cotteaui (Echinoidea, Eoceno inferior) en España. Batalleria 22, 29–33.

Carrasco, J.F., 2017. Presencia de Rhabdocidaris tournali Desor, 1855 (Echinoidea, Eoceno) en España. Batalleria 25, 13–19.

Connell, J.H., 1978. Diversity in tropical rain forests and coral reefs. Science 199, 1302–1310. https://doi.org/10.1126/science.199.4335.1302.

Cotteau, G.H., 1863. Échinides Fossiles des Pyrénées. Libraire de la Société Gélogique de France, Paris (156 pp.).

Cotteau, G.H., 1887. Paléontologie Française ou Description des Fossiles de la France, Échinides Éocènes. Libraire de l'Academie de Médecine, Paris (690 pp.).

Cotteau, G.H., 1889. Échinides recueillis dans la province d'Aragon (Espagne). Ann. Sci. Nat. Zool. Biol. Anim. 8, 1–60.

Desor, E., 1853. Notice sur les Échinides du terrain Nummulitique des Alpes, avec les diagnoses de plusieurs espèces et genres nouveaux. Societe Helvetiques des Sciences Naturelles 38, 270–276.

Duncan, P.M., Sladen, W.P., 1882-1886. Fossil Echinoidea of Western Sind and the Coast of Biluchistan and of the Persian Gulf, from Tertiary formations. Memoirs of the Geological Survey of India, Palaeontologia Indica, Ser.14, 1(3), 1–392.

Dunhill, A.M., Hannisdal, B., Benton, M.J., 2014. Disentangling rock record bias and common-cause from redundancy in the British fossil record. Nat. Commun. 5, 4818. https://doi.org/10.1038/ncomms5818.

Dworschak, P.C., 2000. Global diversity in the Thalassinidea (Decapoda). J. Crustacean Biol. 20, 238–245. https://doi.org/10.1163/1937240X-90000025.

Dworschak, P.C., 2005. Global diversity in the Thalassinidea (Decapoda): an update (1998-2004). Nauplius 13, 57–63.

Eichenseer, H., 1988. Facies geology of late Maastrichtian to early Eocene coastal and shallow marine sediments, Tremp-Graus Basin, northeastern Spain. Ph.D. Thesis, Univ. of Tübingen (273 pp.).

Eichenseer, H., Luterbacher, H., 1992. The marine Paleogene of the Tremp Region (NE Spain)-depositional sequences, facies history, biostratigraphy and controlling factors. Facies 27(1), 119–151.

Ferratges, F.A., Zamora, S., Aurell, M., 2019. A new genus and species of Parthenopidae MacLeay, 1838 (Decapoda: Brachyura) from the lower Eocene of Spain. J. Crustacean Biol. 39(3), 303–311. https://doi.org/10.1093/jcbiol/ruz014.

Ferratges, F.A., Zamora, S., Aurell, M., 2020. Systematics and distribution of decapod crustaceans associated with late Eocene coral buildups from the southern Pyrenees (Spain). Neues Jahrb. Geol. P-A. 296, 79–100. https://doi.org/10.1127/njgpa/2020/0893.

Ferrer, J., 1971. El Paleoceno y Eoceno del borde sur-oriental de la Depresión del Ebro (Cataluña). Mémoires Suisses de Paléontologie 90, 1–70.

Fonnesu, F., 1984. Estratigrafía física y análisis de facies de la secuencia de Figols, entre el rio Noguera Pallaresa e Iscles (prov. de Lérida y Huesca). Ph.D. Thesis Universitat Autonoma de Barcelona, (317 pp.).

Fraaije, R.H., Pennings, H.W., 2006. Crab carapaces preserved in nautiloid shells from the Upper Paleocene of Huesca: Pyrenees, Spain. Rev. Mex. Cienc. Geol. 23, 361–363.

Gaemers, P.A.M., 1978. Biostratigraphy, paleoecology and paleogeography of the mainly marine Ager Formation (Upper PaleoceneLower Eocene) in the Tremp basin, Central South Pyrenees, Spain. Leidse Geologische Mededelingen 51, 151–231.

Garcés, M., López-Blanco, M., Valero, L., Beamud, E., Muñoz, J.A., Oliva-Urcia, B., Vinyoles, A., Arbués, P., Caballero, P., Cabrera, L., 2020. Paleogeographic and sedimentary evolution of the south-pyrenean foreland basin. Mar. Petrol. Geol. 113, 104105. https://doi.org/10.1016/j.marpetgeo.2019.104105.

Goeke, G.D., 1985. Decapod Crustacea: Raninidae. Mémoire Muséum National l'Histoire Naturelle, Series A, Zoologie 133, 205–228.

Gurrea, I., 1999. Nota sobre un equínido fósil no descrito en la península ibérica. Comunicats 8, 3–7.

Hallock, P., Pomar, L., 2008. Cenozoic evolution of larger benthic foraminifers: paleoceanographic evidence for changing habitats. Proceedings of the 11th International Coral Reef Symposium, Ft. Lauderdale, Florida, pp. 16–20.

Hallock, P., Premoli-Silva, I., Boersma, A., 1991. Similarities between planktonic and larger foraminiferal evolutionary trends through Paleogene paleoceanographic changes. Palaeogeogr. Palaeoclimatol. Palaeoecol. 83, 49–64. https://doi.org/10.1016/0031-0182(91)90075-3.

Hammer, Ø., Harper, D.A., Ryan, P.D., 2001. PAST: Paleontological statistics software package for education and data analysis. Palaeontologia electronica 4.(1), 9.

Hannisdal, B., Peters, S.E., 2011. Phanerozoic Earth system evolution and marine biodiversity. Science 334(6059), 1121–1124. https://doi.org/10.1126/science.1210695.

Hay, W.W., De Conto, R., Wold, C.N., Wilson, K.M., Voigt, S., Schulz, M., Wold-Rossby, A., Dullo, W.C., Ronov, A.B., Balukhovsky, A.N., Soeding, E., 1999. Alternative Global Cretaceous Paleogeography. In: Barrera, E., Johnson, C. (Eds.), The Evolution of Cretaceous Ocean/Climate Systems. GSAB Spec. 332. Boulder, Colorado, pp. 1–47.

Hébert, M., 1882. Groupe Nummulitique du Midi de la France. Groupe Nummulitique des Corbières et de la Montagne-Noire. Bull. Soc. Geol. Fr. 3, 364–392.

Hyžný, M., Klompmaker, A.A., 2015. Systematics, phylogeny, and taphonomy of ghost shrimps (Decapoda): a perspective from the fossil record. Arthropod Syst. Phylo. 73(3), 401–437.

Jakobsen, S.L., Feldmann, R.M., 2004. Epibionts on *Dromiopsis rugosa* (Decapoda: Brachyura) from the late Middle Danian limestones at Fakse Quarry, Denmark: novel preparation techniques yield amazing results. J. Paleontol. 78(5), 953–960. https://doi.org/10.1666/0022-3360(2004)078<0953:EODRDB>2.0.CO;2.

Kasinathan, C., Sukumaran, S., Gandhi, A., Boominathan, N., Rajamani, M., 2007. On a rare species of Spanner crab *Ranina ranina* (Crustacea: Brachyura: Raninidae) from Gulf of Mannar, India. J. Mar. Biolo. Assoc. of India 49, 89–90.

Klompmaker, A.A., Hyžný, M., Jakobsen, S.L., 2015. Taphonomy of decapod crustacean cuticle and its effect on the appearance as exemplified by new and known taxa from the Cretaceous–Danian crab *Caloxanthus*. Cretaceous Res. 55, 141–151. https://doi.org/10.1016/j.cretres.2014.11.011.

Klompmaker, A.A., Jakobsen, S.L., Lauridsen, B.W., 2016. Evolution of body size, vision, and biodiversity of coral-associated organisms: evidence from fossil crustaceans in cold-water coral and tropical coral ecosystems. BMC Evol. Biol. 16(1), 132. https://doi.org/10.1186/s12862-016-0694-0.

Klompmaker, A.A., Ortiz, J.D., Wells, N.A., 2013a. How to explain a decapod crustacean diversity hotspot in a mid-Cretaceous coral reef. Palaeogeogr. Palaeoclimatol. Palaeoecol. 374, 256–273. https://doi.org/10.1016/j.palaeo.2013.01.024.

Klompmaker, A.A., Portell, R.W., Frick, M.G., 2017. Comparative experimental taphonomy of eight marine arthropods indicates distinct differences in preservation potential. Palaeontology 60(6), 773–794. https://doi.org/10.1111/pala.12314.

Klompmaker, A.A., Schweitzer, C.E., Feldmann, R.M., Kowalewski, M., 2013b. The influence of reefs on the rise of Mesozoic marine crustaceans. Geology 41, 1179–1182. https://doi.org/10.1130/G34768.1.

Krause Jr, R.A., Parsons-Hubbard, K., Walker, S.E., 2011. Experimental taphonomy of a decapod crustacean: Long-term data and their implications. Palaeogeogr. Palaeoclimatol. Palaeoecol. 312(3-4), 350–362. https://doi.org/10.1016/j.palaeo.2011.03.020.

Luque, J., Feldmann, R.M., Vernygora, O., Schweitzer, C.E., Cameron, C.B., Kerr, K.A., Vega, A., Duque, A., Strange, M., Palmer, A.R., Jaramillo, C., 2019. Exceptional preservation of mid-Cretaceous marine arthropods and the evolution of novel forms via heterochrony. Science advances, 5(4), eaav3875. https://doi.org/10.1126/sciadv.aav3875.

Luterbacher, H.P., Eichenseer, H., Betzler, C., Van Den Hurk, A.M., 1991. Carbonate; Depositional Systems in the Paleogene of the South Pyrenean Foreland Basin: A Sequence-Stratigraphic Approach. Sedimentation, Tectonics and Eustasy: Sea-Level Changes at Active Margins. 391–407. https://doi.org/10.1002/9781444303896.ch21

Madin J.S., Connolly, S.R., 2006. Ecological consequences of major hydrodynamic disturbances on coral reefs. Nature 444, 477–280. https://doi.org/10.1038/nature05328.

Madin, J.S., Hughes, T.P., Connolly, S.R., 2012. Calcification, storm damage and population resilience of tabular corals under climate change. PLoS One 7(10). https://doi.org/10.1371/journal.pone.0046637.

Martinius, A.W., 2011. Contrasting styles of siliciclastic tidal deposition in developing thrust-sheet-top basins – the Lower Eocene of the central Pyrenees (Spain). In: Davis, Jr., R.A., Dalrymple, R.W. (Eds.), Principles of Tidal Sedimentology. Springer, Dordrecht, pp. 473–506.

Massel, S., Done, T., 1993. Effects of cyclone waves on massive coral assemblages on the Great Barrier Reef: meteorology, hydrodynamics and demography. Coral Reefs 12, 153–166.

Miller, K.G., Kominz, M.A., Browning, J.V., Wright, J.D., Mountain, G.S., Katz, M.E., Sugarman, P.J., Cramer, B.S., Christie-Blick, N., Pekar, S.F., 2005. The Phanerozoic record of global sea-level change. Science 310, 1293–1298. https://doi.org/10.1126/science.1116412.

Morsilli, M., Bosellini, F.R., Pomar, L., Hallock, P., Aurell, M., Papazzoni, C.A., 2012. Mesophotic coral buildups in a prodelta setting (Late Eocene, southern Pyrenees, Spain): a mixed carbonate-siliciclastic system. Sedimentology 59, 766–794. https://doi.org/10.1111/j.1365-3091.2011.01275.x

Mutel, M.H., Waugh, D.A., Feldmann, R.M., Parsons-Hubbard, K.M., 2008. Experimental taphonomy of *Callinectes sapidus* and cuticular controls on preservation. Palaios 23(9), 615–623. https://doi.org/10.2110/palo.2008.p08-024r.

Nebelsick, J.H., 2004. Taphonomy of Echinoderms: introduction and outlook. In: Heinzeller, T. Nebelsick, J.H. (Eds.), Echinoderms: Munchen, Taylor & Francis, London, pp. 471–477.

Nebelsick, J.H., Kroh, A., 2002. The stormy path from life to death assemblages: the formation and preservation of mass accumulations of fossil sand dollars. Palaios 17(4), 378–393. https://doi.org/10.1669/0883-1351(2002)017<0378:TSPFLT>2.0.CO;2.

Parsons-Hubbard, K.M., Powell, E.N., Raymond, A., Walker, S.E., Brett, C., Ashtonalcox, K., Shepard, R.N., Krause, R., Deline, B., 2008. The taphonomic signature of a brine seep and the potential for Burgess Shale style reservation. J. Shellfish Res. 27, 227–239. https://doi.org/10.2983/0730-8000(2008)27[227:TTSOAB]2.0.CO;2.

Payros, A., Astibia, H., Cearreta, A., Pereda-Suberbiola, X., Murelaga, X., Badiola, A., 2000. The Upper Eocene South Pyrenean Coastal deposits (Liedena sandstone, navarre): Sedimentary facies, benthic formanifera and avian ichnology. Facies 42(1), 107–131.

Payros, A., Ortiz, S., Millán, I., Arostegi, J., Orue-Etxebarria, X., Apellaniz, E., 2015. Early Eocene climatic optimum: Environmental impact on the North Iberian continental margin. Bulletin 127(11-12), 1632–1644. https://doi.org/10.1130/B31278.1.

Peters, S.E., 2005. Geologic constraints on the macroevolutionary history of marine animals. P. Natl. Acad. Sci-Biol. 102(35), 12326–12331. https://doi.org/10.1073/pnas.0502616102.

Peters, S.E., Heim, N.A., 2011. Stratigraphic distribution of marine fossils in North America. Geology. 39(3), 259–262. https://doi.org/10.1130/G31442.1.

Plaziat, J., 1981. Late Cretaceous to late Eocene paleogeographic evolution of southwest Europe. Paleogeogr. Palaeoclimatol. Palaeoecol. 36, 263–320. https://doi.org/10.1016/0031-0182(81)90110-3.

Plaziat, J.C., Perrin, C., 1992. Multikilometer-sized reefs built by foraminifera (Sol-enomeris) from the early Eocene of the Pyrenean domain (S. France, N. Spain): paleoecologic relations with coral reefs. Palaeogeogr. Palaeoclimatol. Palaeoecol. 96, 195-231. https://doi.org/10.1016/0031-0182(92)90103-C.

Plotnick, R.E., 1986. Taphonomy of a modern shrimp: implications for the arthropod fossil record. Palaios 1, 286–293.

Pomar, L., Baceta, J.I., Hallock, P., Mateu-Vicens, G., Basso, D., 2017. Reef building and carbonate production modes in the west-central Tethys during the Cenozoic. Mar. Petrol. Geol. 83, 261–304. https://doi.org/10.1016/j.marpetgeo.2017.03.015.

Pujalte, V., Caballero, J.I., Schmitz, B., Orue-Etxebarria, X., Payros, A., Bernaola, G., Apellaniz, E., Caballero, F., Robador, A., Serra-Kiel, J., Tosquella, J., 2009. Redefinition of the Ilerdian stage (early Eocene). Geol. Acta. 7(1), 177–194.

Rasser, M.W., Scheibner, C., Mutti, M., 2005. A paleoenvironmental standard section for Early Ilerdian tropical carbonate factories (Corbieres, France; Pyrenees, Spain). Facies 51, 218–232.

Robador, A., Orue-Etxebarria, X., Serra-Kiel, J., 1991. The correlation between biozonation of benthonic and planktonic foraminifera. In Introduction to the early Paleogene of the South Pyrenean Basin. First Meeting IGCP 286: Early Paleogene Benthos, Jaca, Instituto Tecnologico Geomin. España, Madrid. 97–100.

Scheibner, C., Rasser, M.W., Mutti, M., 2007. The Campo section (Pyrenees, Spain) revisited: Implications for changing benthic carbonate assemblages across the Paleocene-Eocene boundary. Palaeogeogr. Palaeoclimatol. Palaeoecol. 248, 145–168. https://doi.org/10.1016/j.palaeo.2006.12.007.

Scheibner, C., Speijer, R.P., 2008. Late Paleocene–early Eocene Tethyan carbonate platform evolution. A response to long- and short-term paleoclimatic change. Earth Science Review. 90, 71–102. https://doi.org/10.1016/j.earscirev.2008.07.002.

Schweitzer, C.E., Feldmann, R.M., 2000. New species of calappid crabs from western North America and reconsideration of the Calappidae sensu lato. J. Paleontol. 74(2), 230–246. https://doi.org/10.1666/0022-3360(2000)074<0230:NSOCCF>2.0.CO;2.

Schweitzer, C.E., Feldmann, R.M., 2015. Faunal turnover and niche stability in marine Decapoda in the Phanerozoic. J. Crustacean Biol. 35, 633–649. https://doi.org/10.1163/1937240X-00002359.

Serra-Kiel, J., Canudo, J.I., Dinares, J., Molina, E., Ortiz, N., Pascual, J.O., Samso, J.M., Tosquella, J., 1994. Cronoestratigrafía de los sedimentos marinos del Terciario inferior de la Cuenca de Graus-Tremp (Zona Central Surpirenaica). Revista de la Sociedad Geológica de España. 7, 273–297.

Silva-Casal, R., Aurell, M., Payros, A., Pueyo, E.L., Serra-Kiel, J., 2019. Carbonate ramp drowning caused by flexural subsidence: the South Pyrenean middle Eocene foreland basin. Sediment. Geol. 393, 1–23. https://doi.org/10.1016/j.sedgeo.2019.105538.

Smith, A.B., Lloyd, G.T., McGowan, A.J., 2012. Phanerozoic marine diversity: rock record modelling provides an independent test of large-scale trends. P. Roy. Soc. B-Bio. Sci. 279(1746), 4489–4495. https://doi.org/10.1098/rspb.2012.1793.

Smith, A.B., Rader, W.L., 2009. Echinoid diversity, preservation potential and sequence stratigraphical cycles in the Glen Rose Formation (early Albian, Early Cretaceous), Texas, USA. Palaeobio. Palaeoenv. 89(1-2), 7–52.

Stickley, C.E., St John, K., Koç, N., Jordan, R.W., Passchier, S., Pearce, R.B., Kearns, L.E., 2009. Evidence for middle Eocene Arctic sea ice from diatoms and ice-rafted debris. Nature 460(7253), 376–379. https://doi.org/10.1038/nature08163.

Tessier, G., Beschin, C., Busulini, A., 2011. New evidence of coral-associated crustaceans from the Eocene of the Vicenza Lessini (NE Italy). Neues Jahrb. Geol. P-A. 260 (2), 211–220. https://doi.org/10.1127/0077-7749/2011/0168.

Tsang, L.M., Schubart, C.D., Ahyong, S.T., Lai, J.C., Au, E.Y., Chan, T.Y., Ng, P.K., Chu, K.H., 2014. Evolutionary history of true crabs (Crustacea: Decapoda: Brachyura) and the origin of freshwater crabs. Mol. Biol. Evol. 31 (5), 1173–1187. https://doi.org/10.1093/molbev/msu068.

Vescogni, A., Bosellini, F.R., Papazzoni, C.A., Giusberti, L., Roghi, G., Fornaciari, E., Dominici, S., Zorzin, R., 2016. Coralgal buildups associated with the Bolca Fossil-Lagerstätten: new evidence from the Ypresian of Monte Postale (NE Italy). Facies. 62(3), 21. https://doi.org/10.1007/s10347-016-0472-x.

Vía-Boada, L., 1973. Datos para el estudio de los crustáceos decápodos del Eoceno circumpirenaico. Pirineos 107, 55–70.

Zachos, J.C., Dickens, G.R., Zeebe, R.E., 2008. An early Cenozoic perspective on greenhouse warming and carbon-cycle dynamics. Nature 451(7176), 279–283. https://doi.org/10.1038/nature06588.

Zachos, J., Pagani, M., Sloan, L., Thomas, E., Billups, K., 2001. Trends, rhythms, and aberrations in global climate 65 Ma to present. Science 292(5517), 686–693. https://doi.org/10.1126/science.1059412.

Zamagni, J., Mutti, M., Košir, A., 2012. The evolution of mid Paleocene-early Eocene coral communities: how to survive during rapid global warming. Palaeogeogr. Palaeoclimatol. Palaeoecol. 317, 48–65. https://doi.org/10.1016/j.palaeo.2011.12.010.

Zamora, S., Aurell, M., Veitch, M., Saulsbury, López-Horgue, M.A., Ferratges, F.A., Arz, J.A., Baumiller, T.K., 2018. Environmental distribution of post-Palaeozoic crinoids from the Iberian and south-Pyrenean basins (NE Spain). Acta Palaeontol. Pol. 63, 779–794. https://doi.org/10.4202/app.00520.2018

Figure 1: **A**: Simplified geological map of the western sector of Tremp-Graus Basin (modified after Serra-Kiel et al., 1994). The red box shows the location of the studied Ramals outcrop (expanded in Figure 2). The red stars of smaller size indicate other localities that supplied complementary material **B**: Synthetic stratigraphic cross-section of the northern margin of the Tremp area during the lower Eocene, with main facies types and the location of the main reefal complexes indicated. Equivalence with the lithostratigraphic units used by Serra-Kiel et al. (1994) is indicated in the legend of the different facies types. Modified from Einchenseer (2003) and Pomar et al. (2017). Coordinates of the sampled outcrops: **1**: 42°21’19.94”N, 0°26’52.69”E; **2**: 42°20’33.29”N, 0°29’01.84”E; **3**: 42°19’33.82”N, 0°29’59.48”E; **4**: 42°19’14.82”N, 0°31’26.14”E; **5**: 42°19’17.92”N, 0°31’45.10”E; **6**: 42°19’10.13”N, 0°33’47.05”E; **7**: 42°19’19.60”N, 0°34’46.21”E; **8**: 42°18’12.66”N, 0°37’22.81”E; **9**: 42°17’47.03”N, 0°37’47.24”E; **10**: 42°17’29.11”N, 0°38’13.69”E; **11**: 42°17’20.35”N, 0°38’40.21”E; **12**:

42°16’54.85”N, 0°39’55.02”E; **13**: 42°16’23.87”N, 0°39’41.08”E; **14**: 42°16’08.42”N, 0°39’45.72”E.

Figure 2: Detailed map of the three members of the Serraduy Formation in Ramals (see Fig. 1.A for location). A, B and C correspond to the different logged sections represented in Figure 3. The field views P1, P2 and P3 show the relationship between reef (red) and inter-reef (orange) facies (see location of the photos in the upper map). The *Alveolina limestones* (dark blue) and the *Riguala marls* (transparent) are the pre- and post-reef deposits respectively. The levels marked with a red star are those that provided the largest number and diversity of decapod crustaceans; the black stars indicate the rock samples collected for thin sections. The acronyms SW and IR refer to the location of the samples (SW: western section; IR: inter-reef).

Figure 3: Correlation of stratigraphic logs (see Fig. 2 for exact location of the logs). The red dashed line shows the boundary between the reef and fore-reef facies to the post-reef facies of the *Riguala marls*. The stars indicate the levels sampled for thin section analysis. Legend: sh: clays; f: fine-grained sandstone; gr: coarse-grained sandstone; m: mudstone; w: wackestone; p: packstone; g: grainstone; fl: floatstone; r: rudstone; bo: boundstone; O.f.r.: Outer fore-reef facies.

Figure 4: Thin section pictures representative of the reef framework. **A** (sample S1): Scleractinian coral framestone with lithophagous bivalves; **B** (sample S8): Framestone with scleractinian corals (1), *Astrocoenia* (2) and *Solenomeris* (3); **C** (sample S6): the wackestone-packstone matrix of the reefal framestone, with discocyclinids, *Acervulina*,

?*Sporolithon* and oysters; **D** (sample S2): Boundstone of tangential section of *Actinacis* with a cavity filled with micritic matrix. Location of samples in figure 3.

Figure 5: Thin section images showing the microfacies representative of the reef mounds (A), inter-reef (B, C, D), inner fore-reef (E, F) and outer fore-reef facies (G, H). **A** (sample SW5C): Scleractinian coral framestones with wackestone matrix; **B** (sample SW6): Poorly-sorted packstone with foraminifera and red algae (coralinacean) encrusting scleractinian coral; **C** (sample IR): Poorly sorted packstone with fragments of foraminifera, molluscs and echinoderms; **D** (sample SW3): Poorly sorted packstone with foraminifera, fragments of red algae and molluscs; **E** (sample ALG): Red coralinacean algae with foraminifera; **F** (sample T): Skeletal packstone with foraminifera; **G** (sample TD): Skeletal packstone with foraminifera and mollusc remains; **H** (sample D-1): Skeletal packstone dominated by foraminifera. Legend: ac: acervulinids; alg: red algae; alv: *Alveolina*; as: *Assilina*; br: bryozoans; cs: calcispheres; di: discocyclinids; ech: echinoderms; mi: miliolids; nu: *Nummulites*; op: *Operculina*; os: ostracods; ro: rotalids. Location of samples in figure 2.

Figure 6: Invertebrate and vertebrate fauna from the Ramals outcrop. **A**: Rostral fragment of *Cylindracanthus* sp. MPZ 2021/3; **B**: indeterminate shark tooth, MPZ 2021/4; **C**: Crocodylia indet. (Eusuchia indet.) MPZ 2021/2; **D**: *Rhyncholites* sp. (Nautiloidea) MPZ 2021/5; **E**: *Arachniopleurus reticulatus* Duncan & Sladen, 1882 MPZ 2021/6; **F**: ?*Ambipleurus* sp. MPZ 2021/7; **G**: ?*Thylechinus frossardi* (Cotteau, 1889) MPZ 2021/8; **H**: *Baueria angelae* Carrasco, 2006, MPZ 2021/9; **I**: *Salenia* sp., MPZ 2021/10; **J-K**: *Cidaris gourdoni* Cotteau, 1889, MPZ 2021/11, MPZ 2021/12 *;* **L-M**:

Fellius pouechi (Cotteau, 1863), MPZ 2021/13, MPZ 2021/14; **N**: *Ditremaster nux* (Desor, 1853), MPZ 2021/15; **O**: *Linthia aragonensis* (Cotteau, 1887), MPZ 2021/16; **P**: ?*Echinocyamus* sp., MPZ 2021/17; **Q**: *Amblypygus dilatatus* Agassiz,1840, MPZ 2021/18; **R**: *Gitolampas cotteaui* (Hébert, 1882), MPZ 2021/19; **S**: *Maretia aragonensis* (Cotteau, 1887), MPZ 2021/20; **T**: ?*Trachyaster* sp., MPZ 2021/21; **U**: *Echinolampas leymeriei* Cotteau, 1863, MPZ 2021/22; **V**: ossicle of ?*Calliderma*, MPZ 2021/23; **W-X**: *Bourgueticrinus* sp., MPZ 2021/24, MPZ 2021/25.

Figure 7: Representatives of decapod crustaceans found in the Ramals outcrop. **A**: Callianassidae indet., MPZ 2021/26; **B**-**C**: *Ctenocheles* cf. *cultellus* (Rathbun, 1935), MPZ 2021/27, MPZ 2021/28; **D**: *Eocalcinus* sp. MPZ 2021/29; **E**: *Pagurus* sp., MPZ 2021/30; **F**: ?*Rhodochirus* sp., MPZ 2021/31; **G**: Paguridae indet., MPZ 2021/32; **H**: indeterminate merus, MPZ 2021/33; **I**: Calappidae indet. 1, MPZ 2021/34; 1 **J1**-**J2**: *Petrolistes* sp., MPZ 2021/36, MPZ 2021/37; **K**: ?Majidae, MPZ 2021/38; **L**: *Ilerdapatiscus guardiae* Artal & Van Bakel, 2018, MPZ 2021/39; **M**: *Aragolambrus collinsi* Ferratges, Zamora & Aurell, 2019, MPZ 2019/211; **N**-**O**: Calappidae indet. 2, MPZ 2021/35, MPZ 2021/40; **P**: Xanthidae indet. 1, MPZ 2021/41; **Q**: Xanthidae indet. 2, MPZ 2021/42; **R**: *Glyphithyreus almerai* Artal & Van Bakel, 2018, MPZ 2021/43; **S**: Xanthilites sp., MPZ 2021/44; **T**: *Litoricola macrodactylus pyrenaicus* (Artal & Vía 1988), MPZ 2021/45; **U**: *Dromilites cf. alpina* Glaessner, 1929, MPZ 2021/46; **V**: *Ranina* sp., MPZ 2021/47; **W**: *Quasilaeviranina* sp., MPZ 2021/48; **X**: *Oscacarpilius rotundus* Artal & Van Bakel, 2018, MPZ 2021/49; **Y**: Dromidae indet., MPZ 2021/50; **Z**: *Eocarpilius ortegai* Artal & Van Bakel, 2018, MPZ 2021/51.

Figure 8: Simplified diagram showing the facies belt distribution. In the reef stage (A), the reefal and inter-reef facies (1), inner fore-reef facies (2), and outer fore-reef facies (3) are differentiated. The development of the reef mound is occasionally controlled by the steep relief generated by the faults affecting the lower unit (*Alveolina limestone*). The red arrows show the dominant offshore transport of skeletal remains by episodic storm-induced currents. In the second stage (B), the reefs were covered by the post-reef *Riguala marls* and there was a significant decrease in the diversity of the benthic fauna.

Figure 9: Pie charts showing the relative abundance and diversity of the different decapod crustacean groups in the different facies. Indeterminate remains were excluded from the analysis.

Figure 10: Distribution of decapod crustacean groups in the different facies. The affinity of each group to the different environments shows how closely they are related to these facies. Plots obtained from Principal Component Analysis (PCA) when processing data with Past4.03. PC1: inner fore-reef; PC2: reefal facies belt; PC3: outer fore-reef.

Figure 11: Rarefaction curves for decapod crustaceans from the three zones with 95 % confidence intervals based on specimens collected between 2018 and 2019. The slopes of the means (middle lines) suggest that inner fore-reef facies preserves the highest diversity.

Figure 12: Shannon index for decapods of the three zones.

Figure 13: Chao1 Index giving the estimated number of species for each site and the standard deviations.

Table 1: Number of specimens and percentage (%) of different decapod crustacean taxa in the different facies of the Ramals outcrop. The reefal facies belt includes both the reef core facies and the inter-reef deposits.

Taxon								Total	% of total
		Specimens	%	Specimens	%	Specimens	%		
Axiidea	Callianassidae		0	2	0.27		0	**2**	**0.22**
	Ctenocheles sp.	5	6.94	456	60.88	41	45.56	**502**	**55.10**
Paguroidea	Paguridae indet. 1		0	1	0.13		0	**1**	**0.11**
	Paguridae indet. 2	1	1.39	5	0.67		0	**6**	**0.66**
	Paguridae indet. 3		0	1	0.13		0	**1**	**0.11**
	Paguridae indet. 4		0	2	0.27		0	**2**	**0.22**
	Paguridae indet. 5		0	2	0.27		0	**2**	**0.22**
	Paguridae indet. 6		0	2	0.27		0	**2**	**0.22**
	? *Paguritta* sp.		0	3	0.40		0	**3**	**0.33**
	Eocalcinus sp.	4	5.56	18	2.40	4	4.44	**26**	**2.85**
	Eocalcinus sp. 2		0	1	0.13		0	**1**	**0.11**
	Petrochirus sp. 1		0	3	0.40		0	**3**	**0.33**
	Petrochirus sp. 2		0	3	0.40		0	**3**	**0.33**
Dromioidea	Dromidae indet. 1		0	9	1.20	1	1.11	**10**	**1.10**
	Dromidae indet. 2		0	1	0.13		0	**1**	**0.11**
	Dromidae indet. 3		0	1	0.13		0	**1**	**0.11**
	Dromidae indet. 4	1	1.39	3	0.40		0	**4**	**0.44**
	Kromtitis sp.		0	2	0.27		0	**2**	**0.22**
Homoloidea	Homolidae indet.		0	2	0.27		0	**2**	**0.22**
Raninoidea	*Antonioranina ripacurtae* (Artal & Castillo, 2005)		0	1	0.13		0	**1**	**0.11**
	Quasilaeviranina sp.		0	1	0.13		0	**1**	**0.11**
	Ranina sp.		0	3	0.40		0	**3**	**0.33**
Aethroidea	*Ilerdapatiscus guardiae* Artal & Van Bakel, 2018	3	4.17	37	4.94	6	6.67	**46**	**5.05**
Calappoidea	Calappidae indet.		0	3	0.40		0	**3**	**0.33**
	Matutidae?		0	1	0.13	1	1.11	**2**	**0.22**
Carpilioidea	*Eocarpilius ortegai* Artal & Van Bakel, 2018	3	4.17	8	1.07	3	3.33	**14**	**1.54**
	Carpilius sp.	6	8.33	6	0.80		0	**12**	**1.32**
	Oscacarpilius rotundus Artal & Van Bakel, 2018	1	1.39	5	0.67	1	1.11	**7**	**0.77**
	Carpiliidae indet.	1	1.39		0		0	**1**	**0.11**
Goneplacoidea	Goneplacidae indet.		0	1	0.13		0	**1**	**0.11**
Hexapodoidea	Hexapodidae indet.		0	1	0.13		0	**1**	**0.11**
Parthenopoidea	*Aragolambrus collinsi* Ferratges. Zamora & Aurell, 2019		0	5	0.67	1	1.11	**6**	**0.66**
Pilumnoidea	*Galenopsis* sp.	3	4.17	1	0.13		0	**4**	**0.44**
Portunoidea	*Litoricola macrodactylus* (Artal & Via, 1988)			1	0.13	10	11.11	**11**	**1.21**
	Ceronectes sp.		0	1	0.13		0	**1**	**0.11**
	Liocarcinus sp.		0	1	0.13		0	**1**	**0.11**

Xanthoidea	*Glyphithyreus almerai* Artal & Van Bakel, 2018		0	9	1.20		0	**9**	**0.99**
	Xanthidae indet. 1		0	1	0.13		0	**1**	**0.11**
	Xanthidae indet. 2		0	2	0.27		0	**2**	**0.22**
	Xanthilites sp.	2	2.78	31	4.14	3	3.33	**36**	**3.95**
	Indet fragments.	28	38.89	40	5.34	16	17.78	**84**	**9.22**
	Morphotype 1	3	4.17	15	2.00	3	3.33	**21**	**2.31**
	Morphotype 2		0	7	0.93		0	**7**	**0.77**
	Morphotype 3	3	4.17	6	0.80		0	**9**	**0.99**
	Morphotype 4		0	5	0.67		0	**5**	**0.55**
	Morphotype 5		0	5	0.67		0	**5**	**0.55**
	Morphotype 6		0	8	1.07		0	**8**	**0.88**
	Morphotype 7		0	8	1.07		0	**8**	**0.88**
	Morphotype 8	1	1.39		0		0	**1**	**0.11**
	Morphotype 9		0	1	0.13		0	**1**	**0.11**
	Morphotype 10		0	7	0.93		0	**7**	**0.77**
	Morphotype 11		0	2	0.27		0	**2**	**0.22**
	Morphotype 12 (carpiliids)	7	9.72	9	1.20		0	**16**	**1.76**
	TOTAL	**72**	**100**	**749**	**100**	**90**	**100**	**911**	**100**

Table 2: Corrected percentages indicating the relative abundance and distribution of main groups of decapod crustaceans the different facies of the Ramals outcrop. The indeterminate taxa are not included.

	Reefal facies bank	%	Inner fore-reef facies	%	Outer fore-reef facies	%	total	%
Axiidea	5	**13.79**	**321**	**65.51**	**29**	**47.54**	354	61.03
Paguroidea	5	**17.24**	**41**	**8.37**	**4**	**6.56**	50	8.62
Dromioidea	**1**	**3.45**	**16**	**3.27**	**1**	**1.64**	18	3.10
Homoloidea	**0**	**0**	**2**	**0.41**	**0**	**0**	2	0.34
Raninoidea	**0**	**0**	**5**	**1.02**	**0**	**0**	5	0.86
Aethroidea	**3**	**10.34**	**37**	**7.55**	**6**	**9.84**	46	7.93
Calappoidea	**0**	**0**	**4**	**0.82**	**1**	**1.64**	5	0.86
Carpilioidea	**11**	**37.93**	**19**	**3.88**	**6**	**9.84**	36	6.21
Hexapodoidea	**0**	**0**	**1**	**0.20**	**0**	**0**	1	0.17
Goneplacoidea	**0**	**0**	**1**	**0.20**	**0**	**0**	1	0.17
Parthenopoidea	**0**	**0**	**5**	**1.02**	**1**	**1.64**	6	1.03
Pilumnoidea	**3**	**10.34**	**1**	**0.20**	**0**	**0**	4	0.69
Portunoidea	**0**	**0**	**3**	**0.61**	**10**	**16.39**	13	2.24
Xanthoidea	**2**	**6.90**	**34**	**6.94**	**3**	**4.92**	39	6.72

Total	29	100	490	100	61	100	580	100

Table 3: Density of crustacean remains obtained after the division of the number of specimens by the surface area of each sector of the outcrop (1: reefal facies; 2: Inner fore-reef facies; and 3: Outer fore-reef facies). Note that the density between representatives of the same group in different areas can vary by several orders of magnitude.

	Zone	Number of specimens	Area (m^2)	Density (specimen/m^2)
Axiidea	1	5	18500	**$2{,}70 \cdot 10^{-4}$**
	2	458	12800	**$3{,}58 \cdot 10^{-2}$**
	3	41	36400	**$1{,}13 \cdot 10^{-3}$**
Paguroidea	1	5	18500	**$2{,}70 \cdot 10^{-4}$**
	2	41	12800	**$3{,}20 \cdot 10^{-3}$**
	3	4	36400	**$1{,}10 \cdot 10^{-4}$**
Dromioidea	1	1	18500	**$5{,}41 \cdot 10^{-5}$**
	2	16	12800	**$1{,}25 \cdot 10^{-3}$**
	3	1	36400	**$2{,}75 \cdot 10^{-5}$**
Homoloidea	1	0	18500	**0**
	2	2	12800	**$1{,}56 \cdot 10^{-4}$**
	3	0	36400	**0**
Raninoidea	1	0	18500	**0**
	2	5	12800	**$3{,}91 \cdot 10^{-4}$**
	3	0	36400	**0**
Aethroidea	1	3	18500	**$1{,}62 \cdot 10^{-4}$**
	2	37	12800	**$2{,}89 \cdot 10^{-3}$**
	3	6	36400	**$1{,}65 \cdot 10^{-4}$**
Calappoidea	1	0	18500	**0**
	2	4	12800	**$3{,}13 \cdot 10^{-4}$**
	3	1	36400	**$2{,}75 \cdot 10^{-5}$**
Carpilioidea	1	11	18500	**$5{,}95 \cdot 10^{-4}$**
	2	19	12800	**$1{,}48 \cdot 10^{-3}$**
	3	4	36400	**$1{,}10 \cdot 10^{-4}$**
Hexapodoidea	1	0	18500	**0**
	2	1	12800	**$7{,}81 \cdot 10^{-5}$**
	3	0	36400	**0**
Goneplacoidea	1	0	18500	**0**
	2	1	12800	**$7{,}81 \cdot 10^{-5}$**
	3	0	36400	**0**
Parthenopoidea	1	0	18500	**0**

	2	5	12800	**$3{,}91 \cdot 10^{-4}$**
	3	1	36400	**$2{,}75 \cdot 10^{-5}$**
Pilumnoidea	1	3	18500	**$1{,}62 \cdot 10^{-4}$**
	2	1	12800	**$7{,}81 \cdot 10^{-5}$**
	3	0	36400	**0**
Portunoidea	1	0	18500	**0**
	2	3	12800	**$2{,}34 \cdot 10^{-4}$**
	3	10	36400	**$2{,}75 \cdot 10^{-4}$**
Xanthoidea	1	2	18500	**$1{,}08 \cdot 10^{-4}$**
	2	43	12800	**$3{,}36 \cdot 10^{-3}$**
	3	3	36400	**$8{,}24 \cdot 10^{-5}$**
Indeterminate	1	42	18500	**$2{,}27 \cdot 10^{-3}$**
	2	113	12800	**$8{,}83 \cdot 10^{-3}$**
	3	19	36400	**$5{,}22 \cdot 10^{-4}$**

Table 4: Diversity metrics and an evenness index for the three studied zones (highest values in bold). The indeterminate taxa are not included.

	Reefal facies	Inner fore-reef facies	Outer fore-reef facies
Specimens	29	**499**	59
Species	11	**39**	10
Superfamilies	7	**14**	9
Simpson's Index of Diversity	**0.877**	0.578	0.708
Shannon–Wiener Index	**2.225**	1.7	1.644
Chao1 Index	14	**52.13**	16
Pielou's evenness index	**0.841**	0.14	0.517

Highlights

- A lower Eocene reef mound complex developed in the mesophotic zone is described
- The invertebrates associated with different facies of the reef complex are documented
- The reef complex includes a rich association of decapods crustaceans that consists of 41 species
- Abundance of different decapod crustacean is quantified from the different facies
- After the demise of the reefs only the decapod *L. macrodactylus pyrenaicus* remained

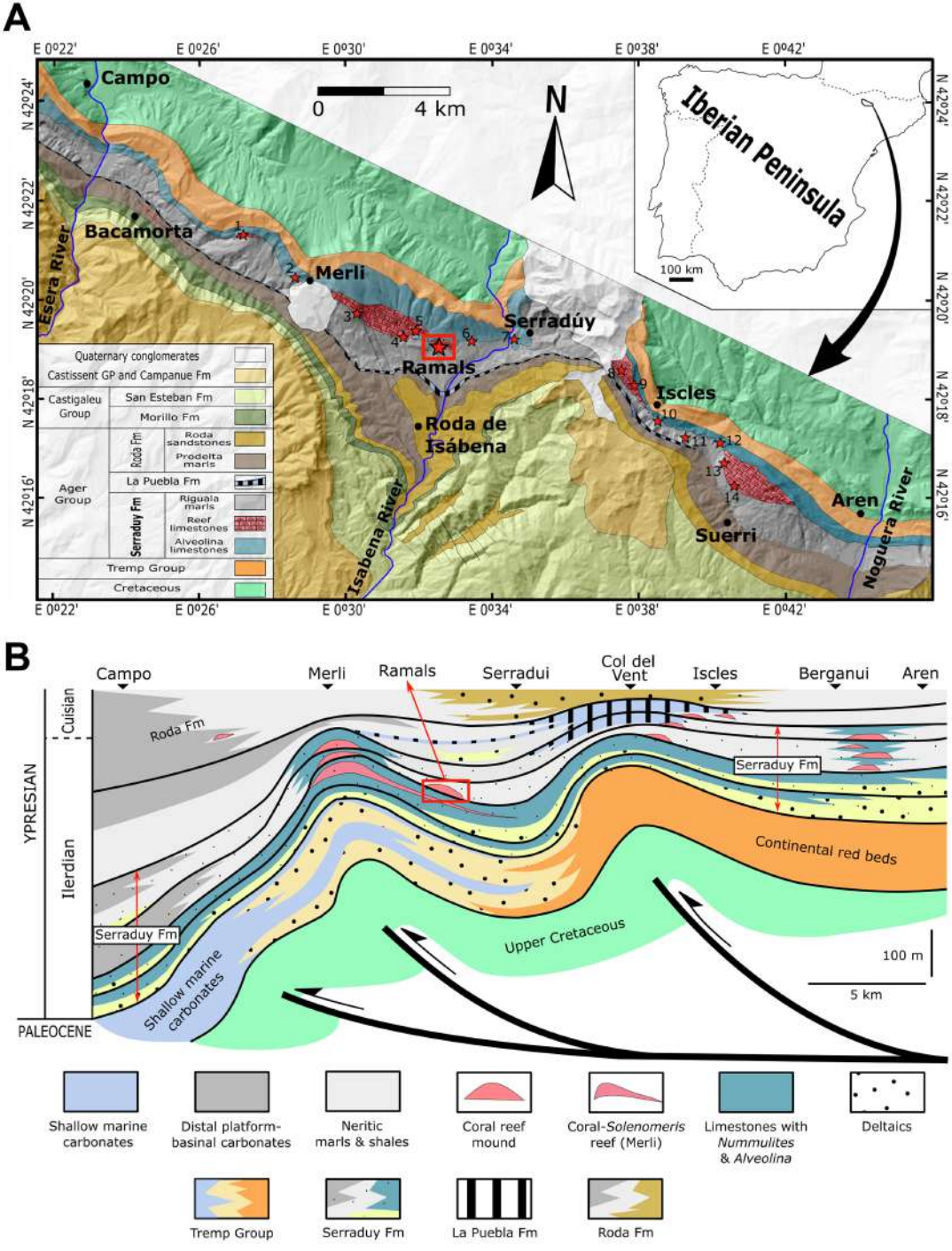
A
E 0°22'
E 0°26'
E 0°30'
E 0°34'
E 0°38'
E 0°42'
N 42°24'
N 42°22'
N 42°20'
N 42°18'
N 42°16'
Campo
Bacamorta
Merli
Serradúy
Ramals
Iscles
Roda de Isábena
Aren
Suerri
Esera River
Isabena River
Noguera River
0
4 km
N
Iberian Peninsula
100 km
Quaternary conglomerates
Castissent GP and Campanue Fm
Castigaleu Group
San Esteban Fm
Morillo Fm
Roda Fm
Roda sandstones
Prodelta marls
Ager Group
La Puebla Fm
Serraduy Fm
Riguala marls
Reef limestones
Alveolina limestones
Tremp Group
Cretaceous
B
Campo
Merli
Ramals
Serradui
Col del Vent
Iscles
Berganui
Aren
Cuisian
YPRESIAN
Ilerdian
PALEOCENE
Roda Fm
Serraduy Fm
Continental red beds
Upper Cretaceous
Shallow marine carbonates
100 m
5 km
Shallow marine carbonates
Distal platform-basinal carbonates
Neritic marls & shales
Coral reef mound
Coral-Solenomeris reef (Merli)
Limestones with Nummulites & Alveolina
Deltaics
Tremp Group
Serraduy Fm
La Puebla Fm
Roda Fm

Figure 1

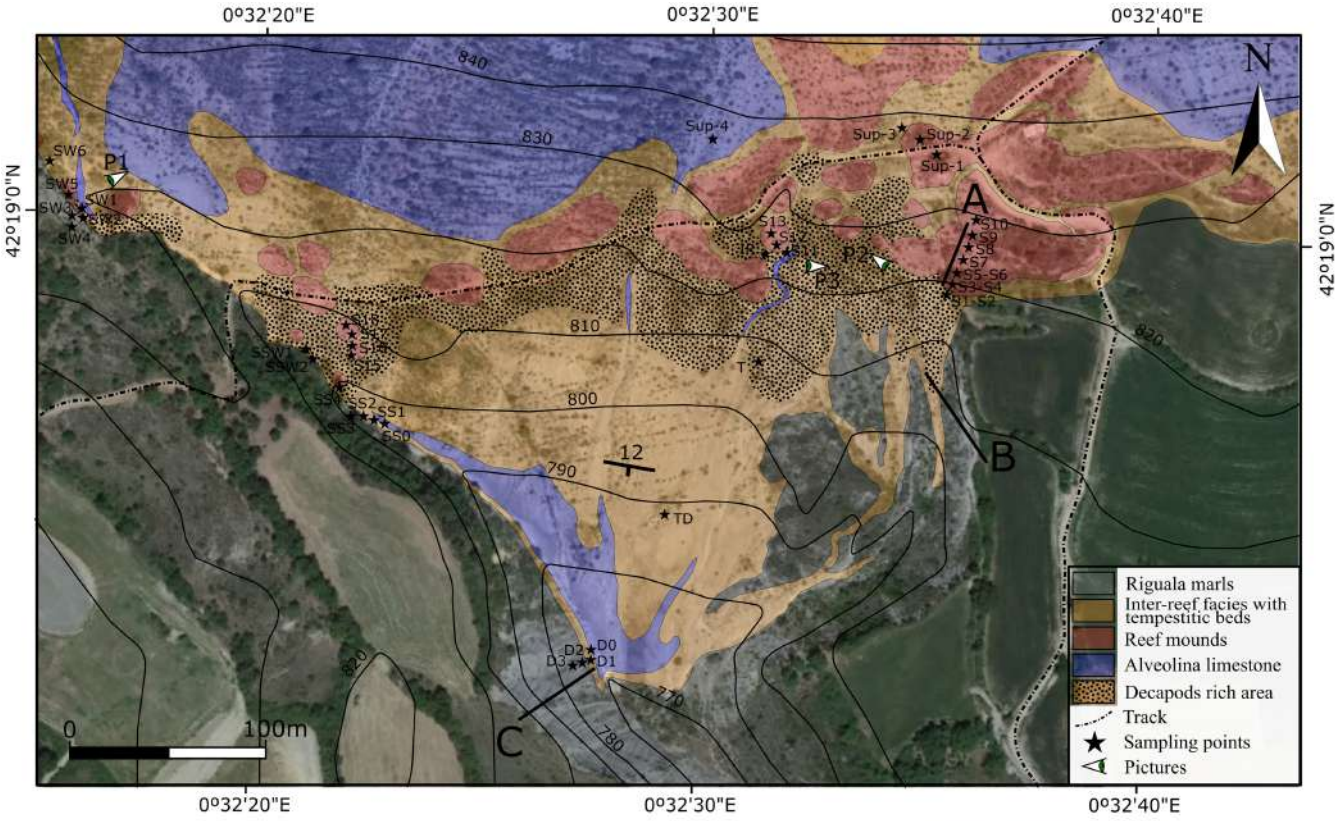
0°32'20"E
0°32'30"E
0°32'40"E
42°19'0"N
N
840
830
820
810
800
790
780
770
Sup-4
Sup-3
Sup-2
Sup-1
P1
P2
A
B
C
12
TD
0
100m
Riguala marls
Inter-reef facies with tempestitic beds
Reef mounds
Alveolina limestone
Decapods rich area
Track
Sampling points
Pictures

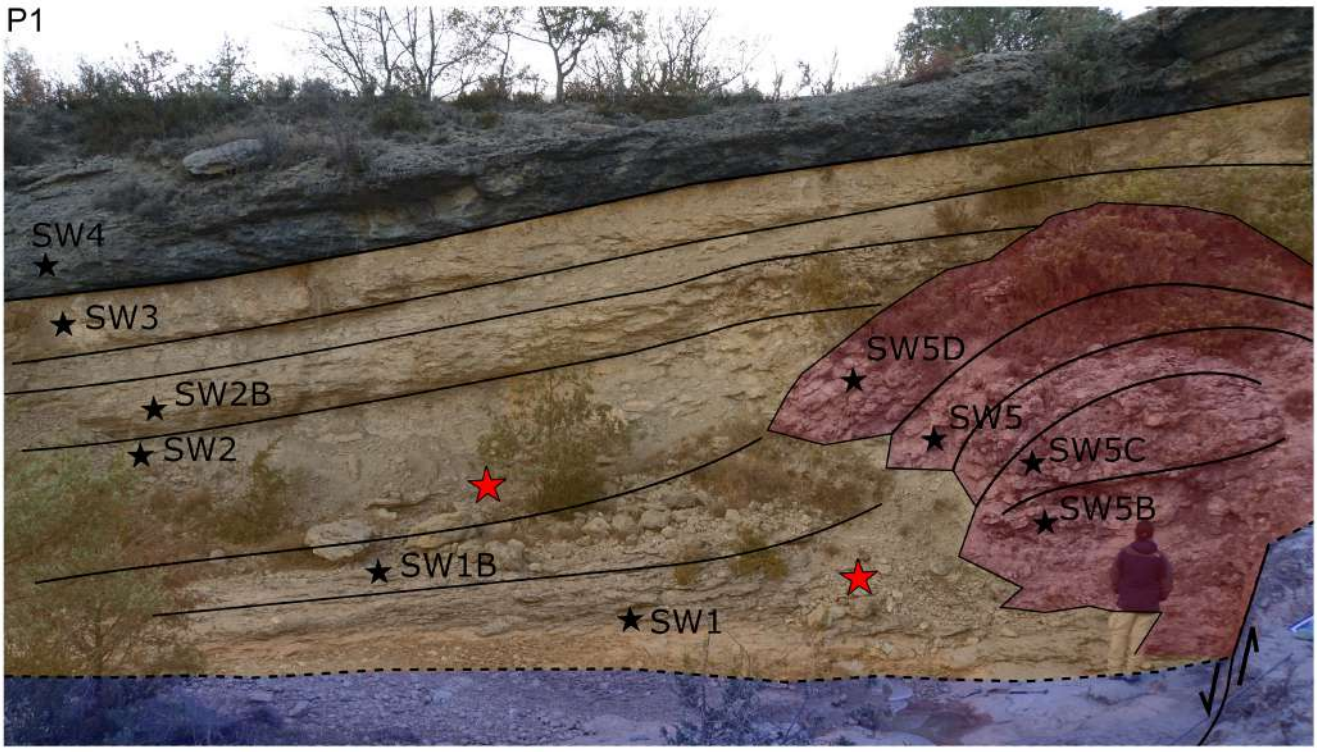
P1
SW4
SW3
SW2B
SW2
SW1B
SW1
SW5D
SW5
SW5C
SW5B


P2

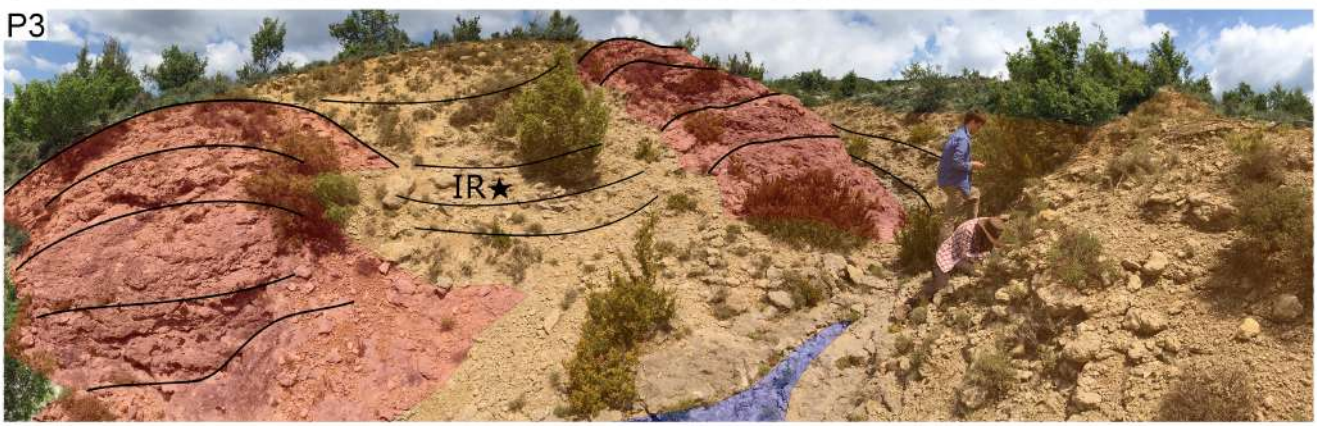
P3
IR

Figure 2

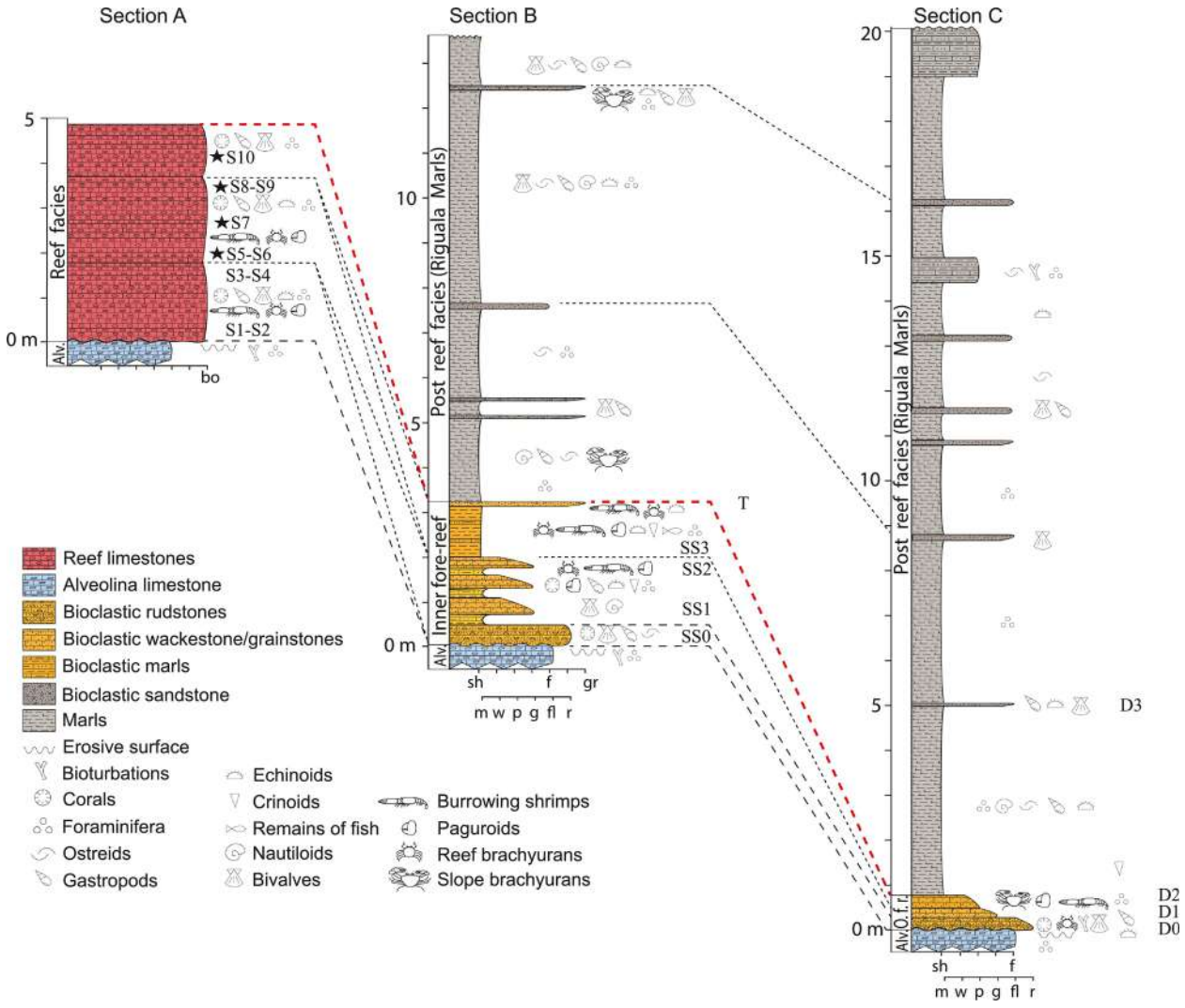
Section A
Section B
Section C
Reef facies
Post reef facies (Riguala Marls)
Inner fore-reef
Alv.
O.f.r.
0 m
5
10
15
20
★S10
★S8-S9
★S7
★S5-S6
S3-S4
S1-S2
bo
T
SS3
SS2
SS1
SS0
D3
D2
D1
D0
sh
f
gr
m w p g fl r
Reef limestones
Alveolina limestone
Bioclastic rudstones
Bioclastic wackestone/grainstones
Bioclastic marls
Bioclastic sandstone
Marls
Erosive surface
Bioturbations
Corals
Foraminifera
Ostreids
Gastropods
Echinoids
Crinoids
Remains of fish
Nautiloids
Bivalves
Burrowing shrimps
Paguroids
Reef brachyurans
Slope brachyurans

Figure 3

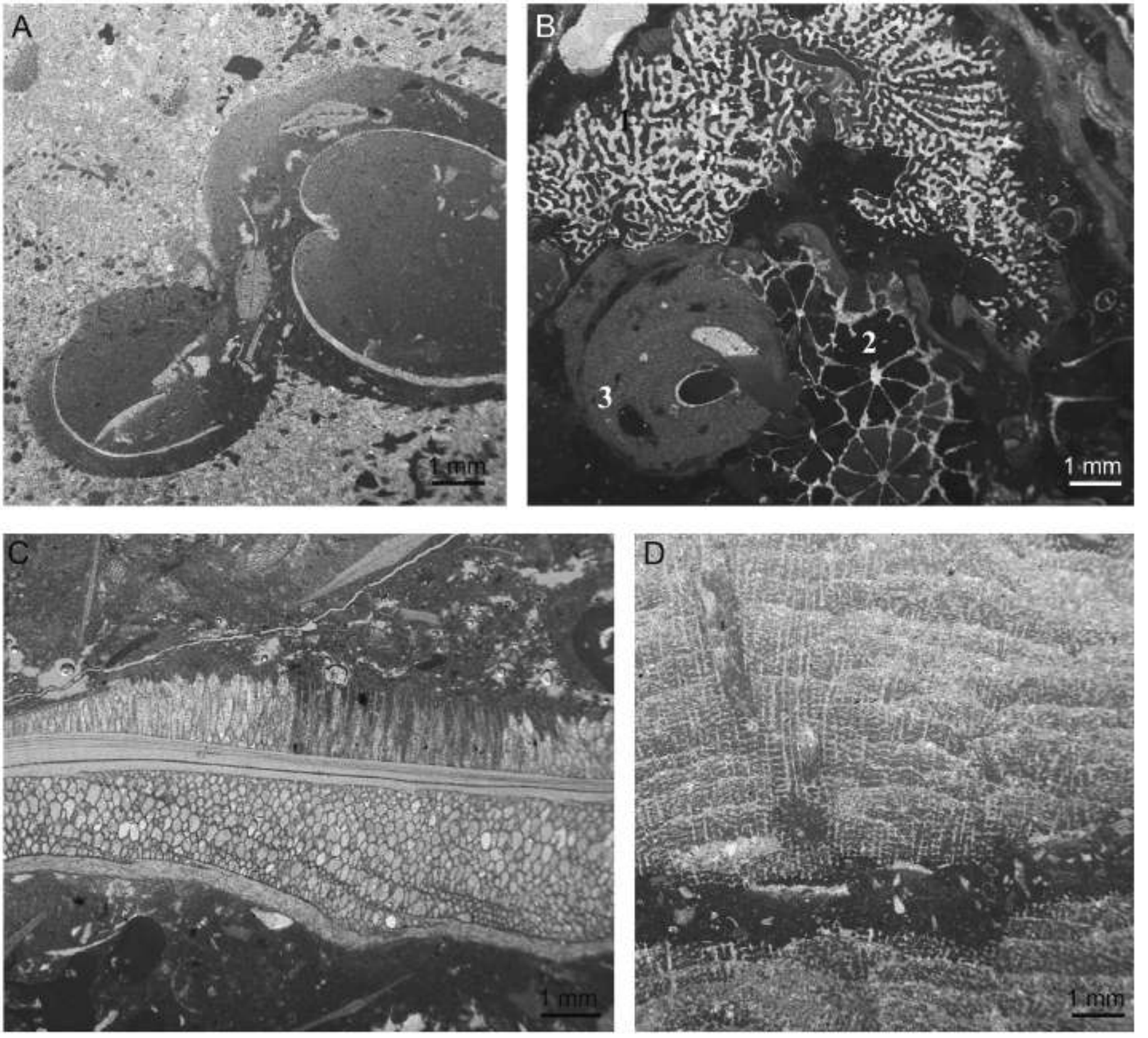

Figure 4

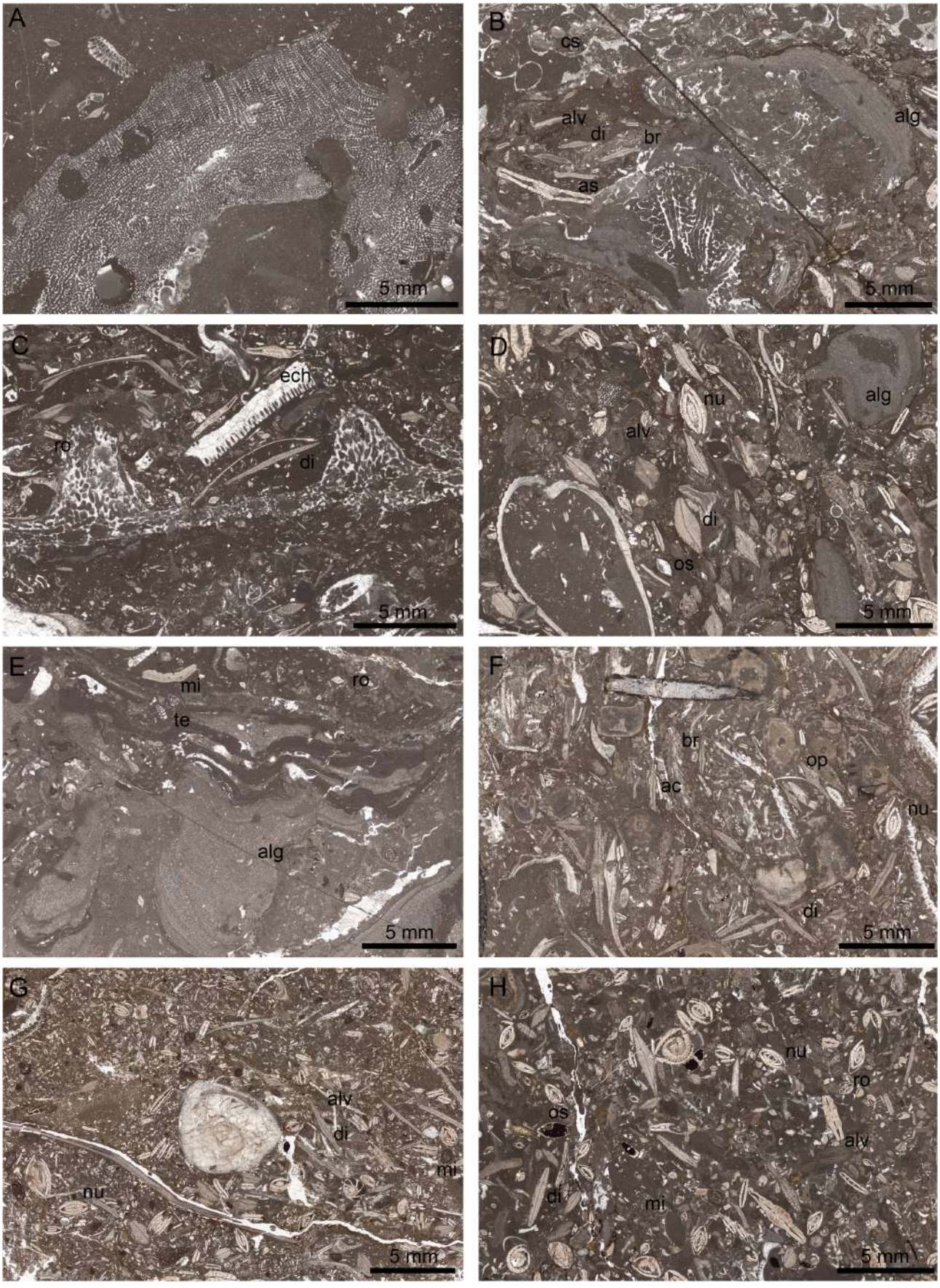
A
5 mm
B
cs
alv
di
br
alg
as
5 mm
C
ech
ro
di
5 mm
D
nu
alg
alv
di
os
5 mm
E
mi
ro
te
alg
5 mm
F
br
op
ac
nu
di
5 mm
G
alv
di
mi
nu
5 mm
H
nu
ro
os
alv
di
mi
5 mm

Figure 5

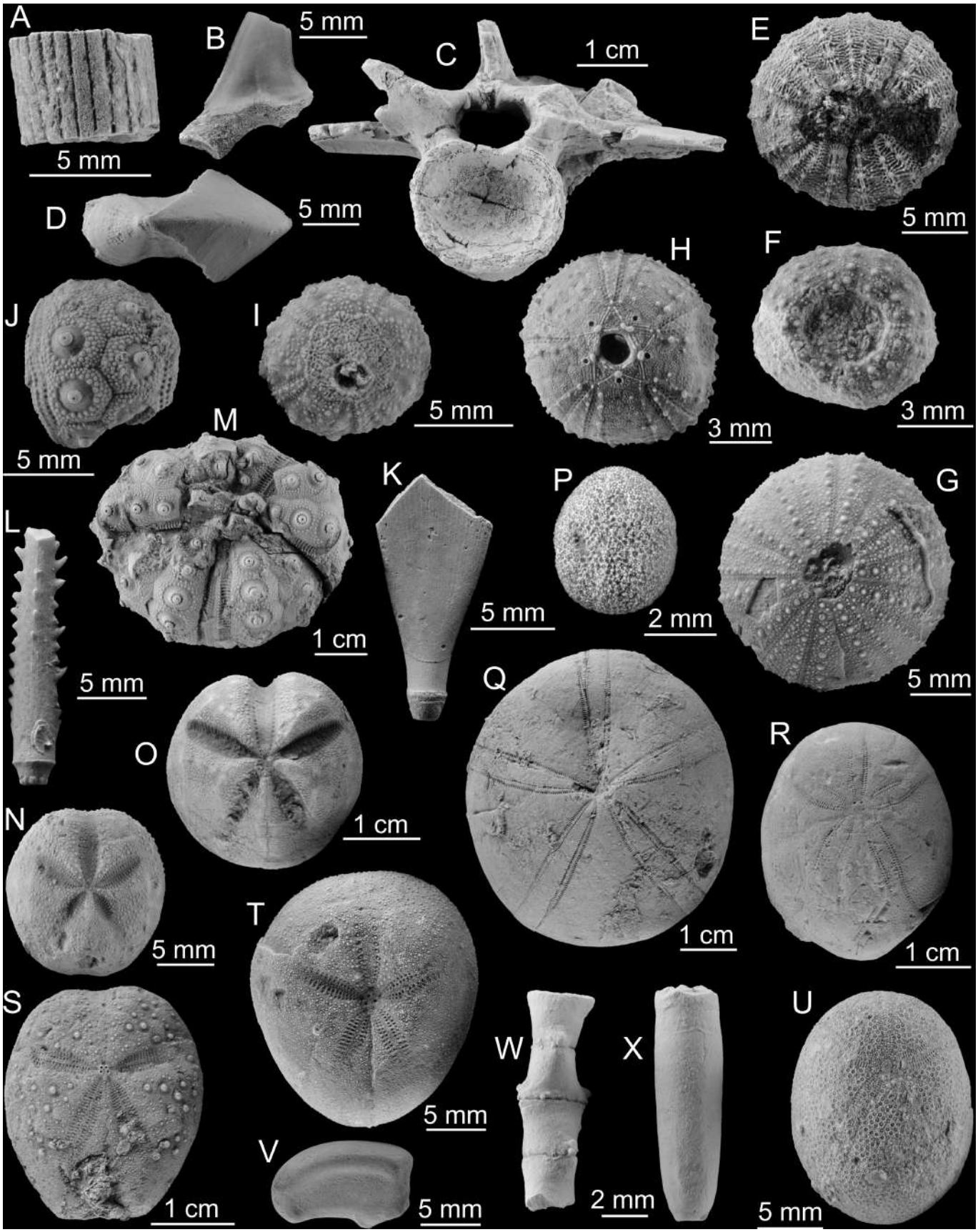
A
5 mm
B
5 mm
C
1 cm
E
5 mm
D
5 mm
H
F
J
I
5 mm
3 mm
3 mm
M
5 mm
K
P
G
L
5 mm
1 cm
5 mm
2 mm
5 mm
Q
R
O
1 cm
N
1 cm
5 mm
T
1 cm
S
5 mm
W
X
U
V
1 cm
5 mm
2 mm
5 mm

Figure 6

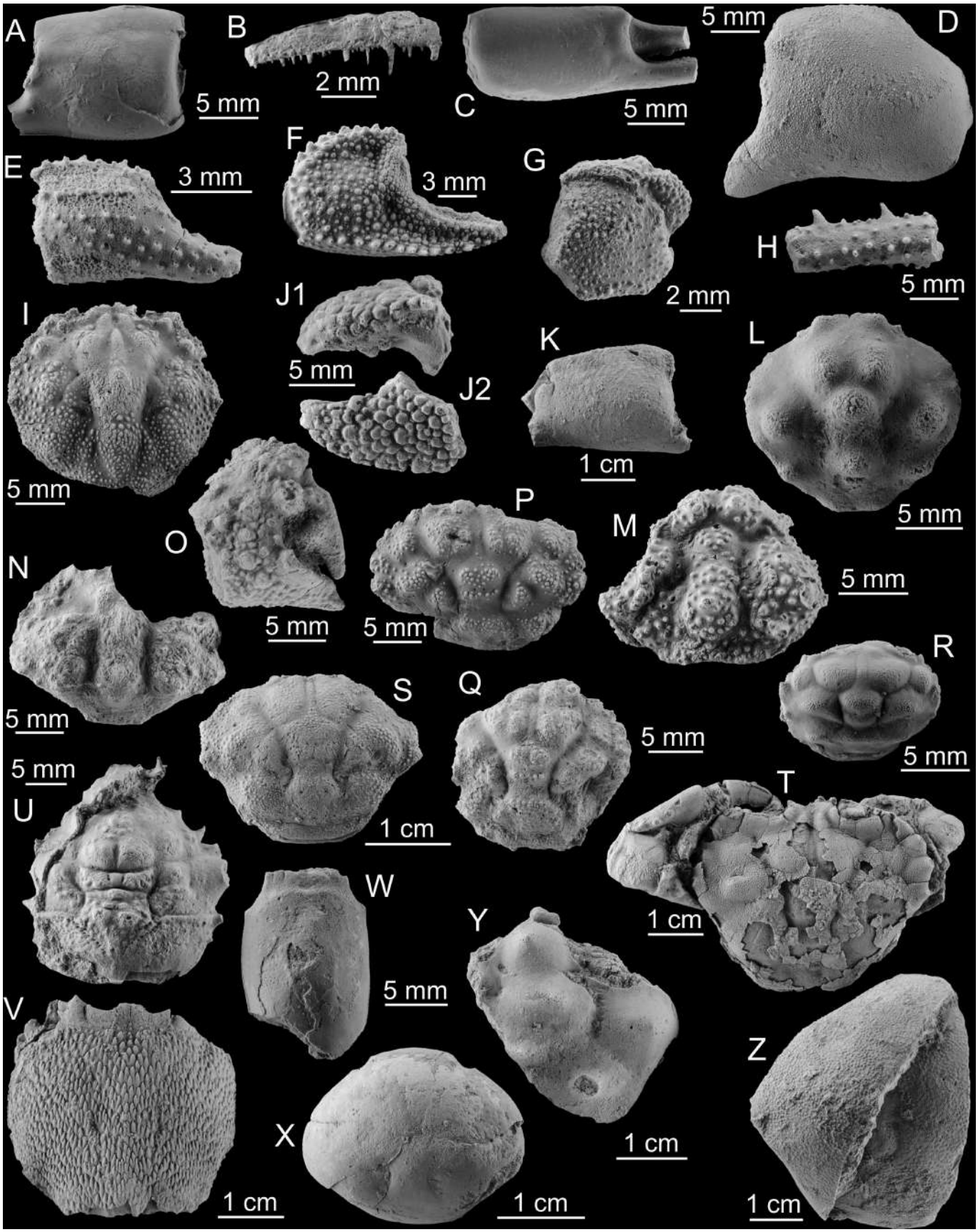
A
5 mm
B
2 mm
C
5 mm
5 mm
D
E
3 mm
F
3 mm
G
2 mm
H
5 mm
I
5 mm
J1
5 mm
J2
K
1 cm
L
5 mm
O
5 mm
P
5 mm
M
5 mm
N
5 mm
R
5 mm
S
1 cm
Q
5 mm
5 mm
U
T
1 cm
W
5 mm
Y
1 cm
V
1 cm
X
1 cm
Z
1 cm

Figure 7

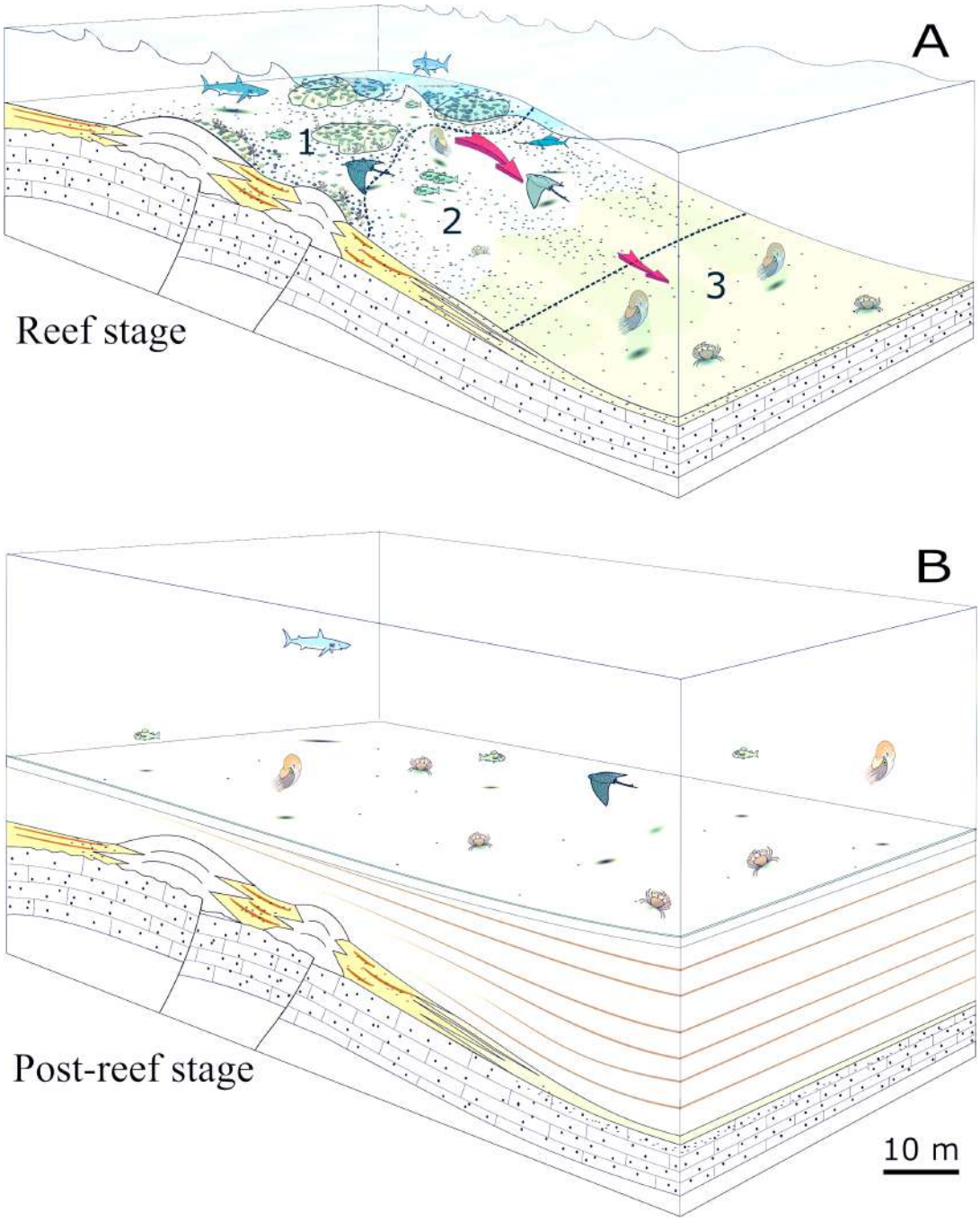

Figure 8

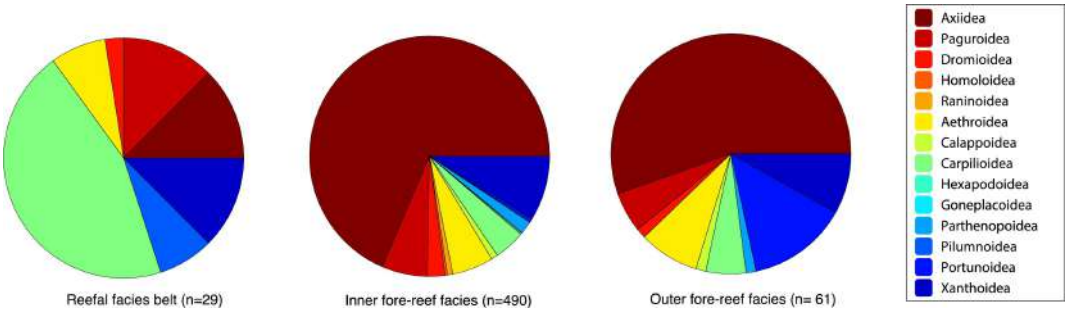
Axiidea
Paguroidea
Dromioidea
Homoloidea
Raninoidea
Aethroidea
Calappoidea
Carpilioidea
Hexapodoidea
Goneplacoidea
Parthenopoidea
Pilumnoidea
Portunoidea
Xanthoidea
Reefal facies belt (n=29)
Inner fore-reef facies (n=490)
Outer fore-reef facies (n= 61)

Figure 9

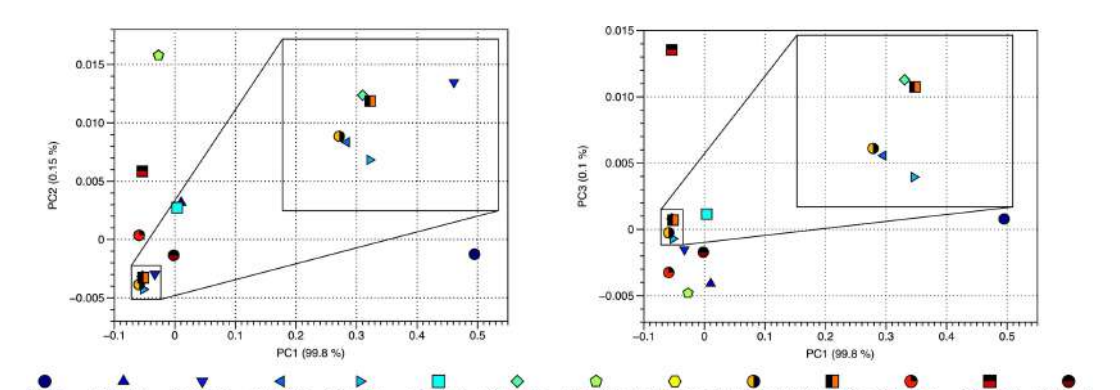
PC2 (0.15 %)
PC1 (99.8 %)
PC3 (0.1 %)
PC1 (99.8 %)
Axiidea
Paguroidea
Dromioidea
Homoloidea
Raninoidea
Aethroidea
Calappoidea
Carpilioidea
Hexapodoidea
Goneplacoidea
Parthenopoidea
Pilumnoidea
Portunoidea
Xanthoidea

Figure 10

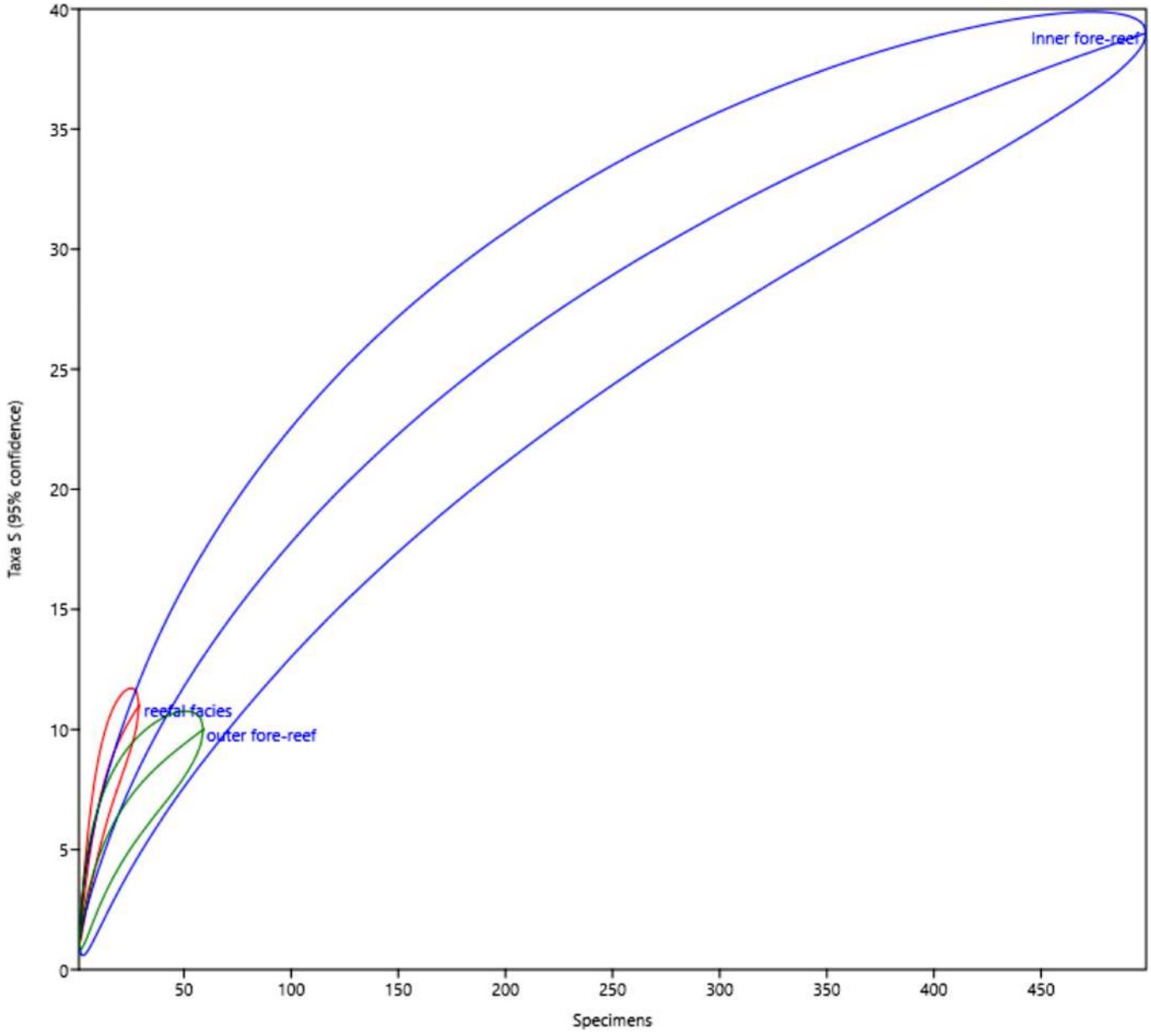
Inner fore-reef
reefal facies
outer fore-reef
Taxa S (95% confidence)
Specimens
0
5
10
15
20
25
30
35
40
50
100
150
200
250
300
350
400
450

Figure 11

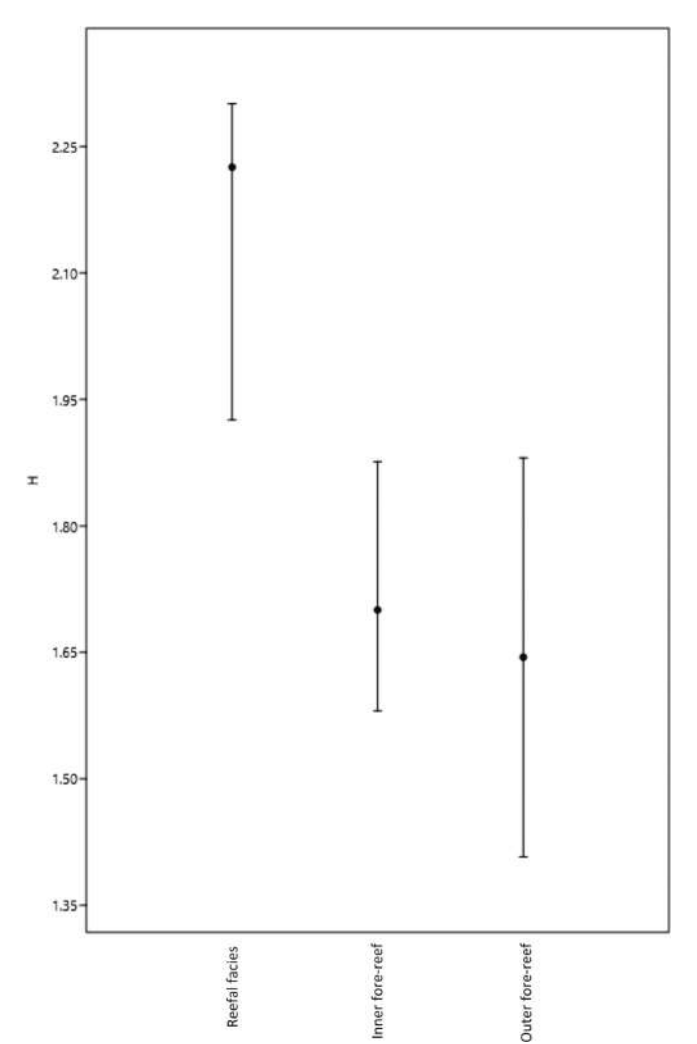
2.25
2.10
1.95
1.80
1.65
1.50
1.35
H
Reefal facies
Inner fore-reef
Outer fore-reef

Figure 12

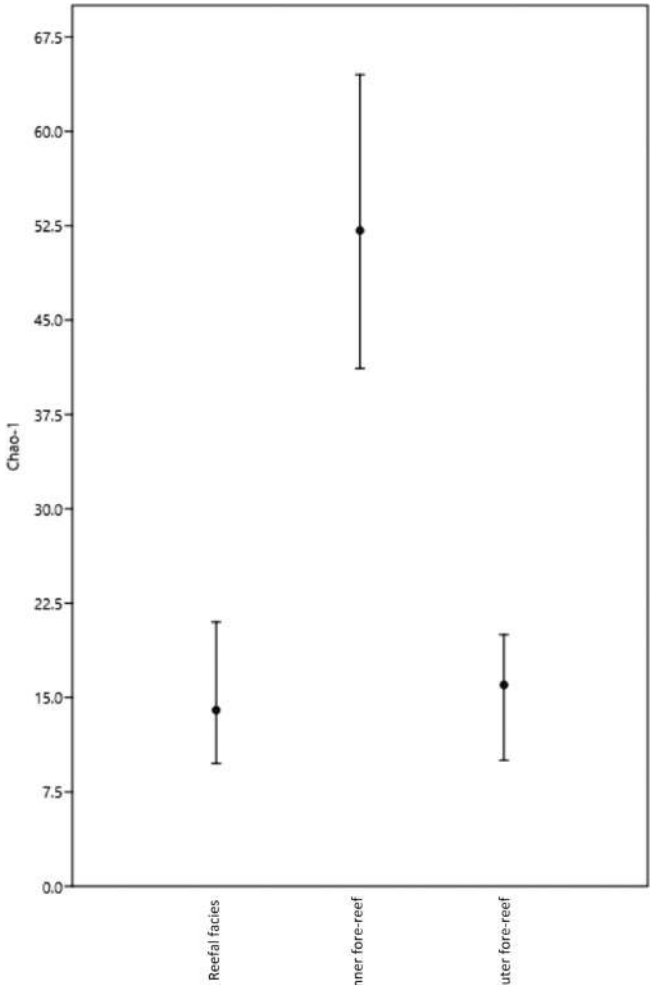
67.5
60.0
52.5
45.0
37.5
30.0
22.5
15.0
7.5
0.0
Chao-1
Reefal facies
Inner fore-reef
Outer fore-reef

Figure 13